TWO-BODY COORDINATE SYSTEM GENERATION USING BODY-FITTED COORDINATE SYSTEM AND COMPLEX VARIABLE TRANSFORMATION

(NASA-CR-153934) TWO-BODY COORDINATE SYSTEM GENERATION USING BODY-FITTED COORDINATE SYSTEM AND COMPLEX VARIABLE TRANSFORMATION M.S. Thesis (Mississippi State Univ., Mississippi State.) 61 p HC A04/MF A01 G3/64 N77-28867 Unclas 39239

by

Walter Serrill Long

A Thesis
Submitted to the Faculty of
Mississippi State University
in Partial Fulfillment of the Requirements
for the Degree of Master of Science
in the Department of Aerophysics and
Aerospace Engineering

Mississippi State, Mississippi

August, 1977

TWO-BODY COORDINATE SYSTEM GENERATION USING BODY-FITTED COORDINATE SYSTEM AND COMPLEX VARIABLE TRANSFORMATION

by

Walter Serrill Long

A Thesis
Submitted to the Faculty of
Mississippi State University
in Partial Fulfillment of the Requirements
for the Degree of Master of Science
in the Department of Aerophysics and
Aerospace Engineering

Mississippi State, Mississippi

August, 1977

TWO-BODY COORDINATE SYSTEM GENERATION USING

BODY-FITTED COORDINATE SYSTEM

AND COMPLEX VARIABLE TRANSFORMATION

by

Walter Serrill Long

Approved:

Professor of Aerospace Engineering and Head, Department of Aerophysics and Aerospace Engineering	Director of Graduate Instruction, College of Engineering
Professor of Aerophysics and Aerospace Engineering (Major Professor)	Dean of the College of Engineering

Dean of the Graduate School

August 1977

ACKNOWLEDGEMENT

The author wishes to express his sincere gratitude to his major professor, Dr. Joe F. Thompson, for his direction and guidance in this masters program. Thanks are also due to Dr. W. Steve Shepard, the graduate advisor, and to Mr. Charles B. Cliett, Professor and Head of the Department of Aerophysics and Aerospace Engineering, for their moral and financial support in this program.

Special thanks are due to Dr. R. N. Reddy for his unending help and encouragement. Finally special thanks go the the author's wife for her support and help in preparing the final manuscript.

The support of NASA, Langley Research Center under Grant NCR-25-001-055 is gratefully acknowledged.

ABSTRACT

Walter Serrill Long, Master of Science, 1977

Major: Aerospace Engineering, Department of Aerophysics and Aerospace Engineering

Title of Thesis: Two-Body Coordinate System Generation Using Body-Fitted Coordinate System and Complex Variable Transformation

Directed by: Dr. Joe F. Thompson

Pages in Thesis: 60 Words in Abstract: 335

ABSTRACT

The purpose of this research was to develop a body-fitted coordinate system for two-element airfoil systems that will be suitable for numerical solutions to the Navier - Stokes equations along with obtaining potential flow results. A general description of the body-fitted coordinate system developed by Thompson, Thames, and Mastin is discussed. This type coordinate system has proved very effective in finding solutions for flows about single-body configurations. The body-fitted coordinate system method can be used to obtain coordinate systems for multi-body configurations also. Using a wing and flap combination, research was conducted to find the best way in which to arrange the airfoil segments on the transformed rectangular plane. Seven separate arrangements were tried and evaluated. Only two of the arrangements showed any success at all. These two coordinate systems are very marginal as they stand now. With the use of coordinate line attraction they could possibly be made more acceptable.

Many different problems were encountered in the two-body

research. One problem was to develop a coordinate system which would have enough coordinate lines to describe the flow field between the two bodies. Another problem was the overlapping of coordinate lines at sharp corners. Two techniques were developed to relieve this problem. One method was to force the coordinate lines not to overlap by controlling the temporary iterative values of X or Y during the iteration process. Another method was to adjust the position of order of the coordinate points describing the bodies.

Because of the lack of success achieved in obtaining a suitable coordinate system in the first seven cases, a new approach was tried. This approach involved using a complex variable transformation of the original body coordinates. The two transformed body coordinates were then entered into the body-fitted coordinate system program and a transformed coordinate system was obtained. This transformed coordinate system was then transformed back to the original physical plane to obtain the physical coordinate system. Three different airfoil combinations were studied. A successful and suitable coordinate system was obtained for each case.

TABLE OF CONTENTS

	Page
ACKNOWLEDGEMENT	iii
ABSTRACT	iv
LIST OF SYMBOLS	vii
LIST OF FIGURES	ix
CHAPTER	
I. INTRODUCTION	1
II. BODY-FITTED CURVILINEAR COORDINATE SYSTEM	3
A. GENERAL DISCUSSION	3
B. REGIONS WITH TWO-BODIES	7
III. PROBLEMS ASSOCIATED WITH MULTIBODY COORDINATE SYSTEMS	9
IV. COMPLEX VARIABLE TRANSFORMATION	13
V. CONCLUSIONS AND RECOMMENDATIONS	22
FIGURES	23
BIBLIOGRAPHY	50

LIST OF SYMBOLS

Symbol	
C	Complex constant
C_I	Imaginary part of C
C_R	Real part of C
R	Physical region
R^*	Transformed region
X	Non-dimensional physical coordinate
Y	Non-dimensional physical coordinate
Z	Complex variable in physical plane
α	Coordinate transformation parameter
β	Coordinate transformation parameter
γ	Coordinate transformation parameter
Γ	Contour in physical plane
Γ^*	Contour in transformed plane
δ	Acceleration parameter
ε	Convergence criteria for given iteration
η	Non-dimensional transformed coordinate
η_1	Pertaining to body contour
η_2	Pertaining to outer boundary contour
ξ	Non-dimensional transformed coordinate
ζ	Complex variable in transformed physical plane
∞	Pertaining to infinity boundary

Subscripts

I,J	Denotes field position in (ξ,η) plane
L.E.	Pertains to airfoil leading edge
O	Pertains to original physical plane
T	Pertains to transformed physical plane
T.E.	Pertains to airfoil trailing edge
XX	Second X partial derivative
YY	Second Y partial derivative
η	First η partial derivative
$\eta\eta$	Second η partial derivative
ξ	First ξ partial derivative
$\xi\xi$	Second ξ partial derivative
$\xi\eta$	Second cross-partial derivative

LIST OF FIGURES

Page

Figure 1. Field Transformation - Single Body. 23

Figure 2. Field Transformation - Two Bodies 24

Figure 3a. Airfoil Trailing Edge With Overlapping Coordinate Lines. 25

Figure 3b. Airfoil Trailing Edge Without Overlapping Coordinate Lines. 25

Figure 4a. Transformed Rectangular Plane View of NACA 64_3-418 Wing-Flap Combination (1st Case). 26

Figure 4b. NACA 64_3-418 Wing-Flap Configuration. 26

Figure 5. Physical Plane Coordinate System of NACA 64_3-418 Wing-Flap Configuration (1st Case) 27

Figure 6. Transformed Rectangular Plane View of NACA 64_3-418 Wing-Flap Combination (2nd Case). 28

Figure 7. Physical Plane Coordinate System of NACA 64_3-418 Wing-Flap Configuration (2nd Case). 29

Figure 8. Physical Plane Coordinates of NACA 64_3-418 Wing-Flap Configuration (Enlarged View). 30

Figure 9. Transformed Physical Plane Coordinates of NACA 64_3-418 Wing-Flap Configuration 31

Figure 10. Transformed Rectangular Plane View of transformed NACA 64_3-418 Wing-Flap Coordinates 32

Figure 11. Transformed Physical Plane Coordinate System of NACA 64_3-418 Wing-Flap Configuration. 33

Figure 12. Physical Plane Coordinate System of NACA 64_3-418 Wing-Flap Configuration. 34

Figure 13. Expanded View of Physical Plane Coordinate System of NACA 64_3-418 Wing-Flap. 35

LIST OF FIGURES
(Cont.)

Page

Figure 14. Physical Plane View of Modified NACA 64_3-418 Wing-Flap Configuration. 36

Figure 15. Transformed Physical Plane of Modified Wing-Flap . . 37

Figure 16. Transformed Rectangular View of Transformed Modified Wing-Flap Coordinates 38

Figure 17. ξ-line Overlap at T.E. 39

Figure 18. ξ-line Overlap at T.E. Corrected 39

Figure 19. Transformed Physical Plane Coordinate System of Modified Wing-Flap Configuration 40

Figure 20. Physical Plane Plot of Modified Wing-Flap Coordinate System. 41

Figure 21. Expanded View of Physical Plane Plot of Modified Wing-Flap Coordinate System. 42

Figure 22. Wing-Slat Configuration. 43

Figure 23. Transformed Physical Plane Diagram of Wing-Slat Configuration. 44

Figure 24. Transformed Rectangular Plane View of Wing-Slat Configuration 45

Figure 25. Slat T.E. With η-line Overlap. 46

Figure 26. Slat T.E. Without η-line Overlap 46

Figure 27. Transformed Physical Plane View of Wing-Slat Configuration 47

Figure 28. Physical Plane Plot of Wing-Slat Coordinate System. 48

Figure 29. Expanded View of Physical Plane Plot of Wing-Slat Coordinate System. 49

I. INTRODUCTION

In the past few years there has been increasing interest in developing numerical solutions to the time-dependent, incompressible Navier-Stokes equations. Originally the research began by developing solutions to very simple body configurations such as the flat plate and circular cylinder. In these cases a simple Cartesian coordinate system or polar coordinate system could be used to obtain the numerical solutions. However, as more complex and complicated geometric shapes came under investigation the need for a more general and better coordinate system became evident.

There have been many different approaches made in an attempt to generate the perfect coordinate system. Some investigators have tried the technique of conformal mapping. Others such as Thompson and his co-workers decided on a different approach. This was to generate a curvilinear coordinate system which would have some coordinate line coincident with each boundary of the physical region of interest. This type of coordinate system proved to be succesful and was referred to as the body-fitted coordinate system. Many different flow solutions over single body configurations have been obtained by utilizing this body-fitted coordinate system.

There have been few attempts to obtain solutions over multi-body configurations and the success of those that have been tried has been limited. The major reason is that a suitable coordinate system for these configurations has not been achieved. This research is concerned mainly with generating acceptable coordinate

systems for two-body configurations. The first method to be tried was to use the body-fitted coordinate system technique to obtain the best system. This technique alone did not produce very good results, so another approach was investigated.

This new approach involved using a combination of the body-fitted coordinate system procedure and a complex variable transformation method that has been used successfully in conformal mapping.

The computer used in this research was a UNIVAC 1106. The plots obtained of the different coordinate systems were plotted by a GOULD 4800 plotter.

II. BODY-FITTED CURVILINEAR COORDINATE SYSTEM

This section is concerned with the development of the type of coordinate system used in this research. This type of boundary-fitted coordinate system may be generated for general, multi-connected, two dimensional regions. The basic foundation of this method of generating body-fitted coordinate systems was laid by Thompson, Thames, and Mastin [1]. A very thorough and detailed discussion of the method that has been used is given by Thames [2]. Therefore, an in depth discussion of the techniques involved will not be given. However, an overview of the whole development process and details to specifics concerned in this research will be discussed in this section.

A. GENERAL DISCUSSION

The major purpose in numerically generating a curvilinear coordinate system is to have some coordinate line coincident with each boundary of the physical region of interest. In this case an airfoil, circular cylinder, or an airfoil and attached flap or slat may be the inner boundary and a large circle representing infinity may be the outer boundary.

Suppose for example that the two-dimensional, doubly-connected region, R, bounded by an inner airfoil and outer circle is to be transformed onto a rectangular region, R*, as shown in Figure 1. It is required that Γ_1 map onto Γ_1*, Γ_2 map onto Γ_2*, Γ_3 onto Γ_3*, and Γ_4 onto Γ_4*. Region R is refered to as the physical plane in X and Y, and region R* is the transformed reetangular plane

in ξ and η. It can be seen that the transformed boundaries (Γ_1* and Γ_2*) become constant coordinate lines(η-lines) in the transformed plane. The contours Γ_3 and Γ_4 represent an arbitrary cut in the physical region R. These contours are coincident in the physical plane and connect Γ_1 and Γ_2. These contours are refered to as reentrant boundaries in the transformed plane.

In order to achieve having coincident coordinate line and boundary, the curvilinear coordinates must be taken to be solutions of an elliptic partial differential system with constant values of one of the curvilinear coordinates, η, specified as Dirichlet boundary conditions on each boundary. The values of the other coordinate, ξ, is specified in a monotonic variation over a boundary as Dirichlet boundary conditions, or are determined by Neumann boundary conditions thereon.

The generating elliptic system used in this case is Laplace's equation.

$$\xi_{xx} + \xi_{yy} = 0 \tag{2.1 a}$$

$$\eta_{xx} + \eta_{yy} = 0 \tag{2.1 b}$$

with Dirichlet boundary conditions

$$\begin{bmatrix} \xi \\ \eta \end{bmatrix} = \begin{bmatrix} \xi_1 \ (x,y) \\ \eta_1 \end{bmatrix} , \ [x,y] \ \varepsilon \ \Gamma_1 \tag{2.1 c}$$

$$\begin{bmatrix} \xi \\ \eta \end{bmatrix} = \begin{bmatrix} \xi_2 \ (x,y) \\ \eta_2 \end{bmatrix} , \ [x,y] \ \varepsilon \ \Gamma_2 \tag{2.1 d}$$

where η_1 and η_2 are constant and $\xi_1(X,Y)$ and $\xi_2(X,Y)$ are specified, non-constant functions on Γ_1 and Γ_2 respectively. Γ_1 and Γ_2 correspond to the inner and outer boundaries respectively in the physical plane or X,Y plane. ξ and η are the variables in the transformed rectangular plane.

Since it is desired to perform all numerical computations in the rectangular transformed plane, the dependent and independent variables are interchanged to yield the new coupled system of equations.

$$\alpha X_{\xi\xi} - 2\beta X_{\xi\eta} + \gamma X_{\eta\eta} = 0 \tag{2.2a}$$

$$\alpha Y_{\xi\xi} - 2\beta Y_{\xi\eta} + \gamma Y_{\eta\eta} = 0 \tag{2.2b}$$

where

$$\alpha = X_\eta^2 + Y_\eta^2 \tag{2.2c}$$

$$\beta = X_\xi X_\eta + Y_\xi Y_\eta \tag{2.2d}$$

$$\gamma = X_\xi^2 + Y_\xi^2 \tag{2.2e}$$

with the transformed boundary conditions

$$\begin{bmatrix} X \\ Y \end{bmatrix} = \begin{bmatrix} f_1(\xi,\eta_1) \\ f_2(\xi,\eta_1) \end{bmatrix}, \quad [\xi,\eta_1] \in \Gamma_1^* \tag{2.2f}$$

$$\begin{bmatrix} X \\ Y \end{bmatrix} = \begin{bmatrix} g_1 \ (\xi, \ \eta_2) \\ g_2 \ (\xi, \ \eta_2) \end{bmatrix}, [\xi, \ \eta_2] \ \varepsilon \ \Gamma_2^* \qquad (2.2 \ g)$$

Where Γ_1^* and Γ_2^* are the inner and outer boundaries in the transformed rectangular plane. The function $f_1 \ (\xi, \ \eta_1)$, $f_2 \ (\xi, \ \eta_1)$, $g_1 \ (\xi, \ \eta_2)$, $g_2 \ (\xi, \ \eta_2)$ are specified by the known shape of the contours Γ_1 and Γ_2 and the specified distribution of ξ theron.

Equations (2.2) are a quasi-linear elliptic system for the physical coordinate functions, $X \ (\xi, \ \eta)$ and $Y \ (\xi, \ \eta)$, in the transformed plane. This is the basic set of equations used to numerically generate the desired coordinate system. The numerical procedure involved is described briefly as follows. Second order central difference expressions are used to approximate all derivatives in the transformed equations (2.2 a,b). A set of non-linear simultaneous difference expressions are used to approximate all derivatives in the transformed equations (2.2 a,b). A set of non-linear simultaneous difference equations are produced. This set of simultaneous equations are then solved by utilizing point SOR (successive overrelaxation) iteration techniques.

Control over the spacing of the curvilinear coordinate lines in the field in order to concentrate more linear in the region of expected high gradients can also be accomplished. This is accomplished by varying the elliptic system (2.2). A summary of this technique is given by Thames [2] and a more thorough explanation is given by Thompson, Thames, and Mastin [1]

For any shape boundaries the numerical generation of the coordinate system is done automatically. The only requirement is

the input of the points on the boundaries.

B. REGIONS WITH TWO - BODIES

This research is specifically concerned with obtaining a numerical solution of the Navier-Stokes equation for arbitrary two-dimensional multi-element airfoils. To be more specific, it is concerned with two airfoils (i.e., a wing and flap combination). In order to accomplish this, a suitable coordinate system has to be developed for the two-body configuration.

The basic theory, procedure, and method discussed previously for the single element airfoil may be extended to regions involving more than one body. One transformation for two bodies is shown in Figure 2. This is only one of many different ways in which two-bodies can be transformed to the transformed planes. Other configurations are given in reference [2]. These will be discussed in more detail in a later chapter. The bodies in Figure 2 are connected with one arbitrary cut and an additional cut joins one of the body contours to the outer boundary. The main difference in this case is that there is an additional cut between the two bodies, Γ_5 and Γ_6. In the transformed plane these become the re-entrant segments Γ_5^* and Γ_6^*. The coordinate functions and their derivatives are continuous across these boundaries. Also body number 2 is defined by the union of Γ_7^* and Γ_8^* in the transformed plane.

The boundary-fitted coordinates for the two-body transformation are also determined by the solution of the set of equations (2.2) but now there are these added boundary conditions required

to define the additional body.

$$\begin{bmatrix} X \\ Y \end{bmatrix} = \begin{bmatrix} h_1 \ (\xi, \ \eta_1) \\ h_2 \ (\ \xi, \ \eta_1) \end{bmatrix}, \ [\xi, \ \eta_1] \ \varepsilon \ \Gamma_7^*$$

$$\begin{bmatrix} X \\ Y \end{bmatrix} = \begin{bmatrix} q_1 \ (\xi, \ \eta_1) \\ q_2 \ (\xi, \ \eta_1) \end{bmatrix}, \ [\xi, \ \eta_1] \ \varepsilon \ \Gamma_8^*$$

The boundary conditions cannot be defined along the reentrant boundaries Γ_3^*, Γ_4^*, Γ_5^*, and Γ_6^* since they are the field points on the cut. Coordinate line attraction can also be utilized with the two-body transformation.

III. PROBLEMS ASSOCIATED WITH MULTIBODY COORDINATE SYSTEMS

There are many problems that are encountered in obtaining suitable coordinate systems for one-body configurations. However, this research deals with obtaining coordinate systems for two-body configurations. The same problems that can be expected in the one-body case may also be expected in the the two-body case and could possibly be compounded. The number of difficulties encountered in the two-body case may be expected because of the complicated geometry of the multiconnected domain.

One of the areas of concern is the region that lies between the two airfoils. It is known that the interaction of the flow between the two airfoils produces large perturbations to the flow field. Therefore accurate results need to be obtained in this region. In order to achieve this, there must be a concentration of many coordinate lines in this area. This requirement can be achieved, but in doing so other problems must be dealt with.

One of these problems is to select and generate the proper initial guess of the coordinate system. This is not a very easy or intuitive chore to accomplish. There are many types of initial guesses that may be tried. Trial and error is about the only way to find out which one best suits the configuration being studied.

A problem that may arise from having an imperfect initial guess is that of coordinate lines overlapping each other. This condition occurs most prevantly on airfoils with sharp trailing edges. This problem has been dealt with in two ways,

One method is to adjust the point spacing on the airfoil that is affected, or to rearrange the order in which the airfoil points are read into the coordinate system program. The second method is a little more specific and involved, but has proved very effective. Suppose for instance that overlap was occurring along a certain ξ-line in the X- direction as shown in Figure 3a which is the trailing edge of some airfoil. This overlap may be eliminated by checking to see if the temporary value of X evaluated at (I,J) is less than or equal to the value of X at (I,J-1). If this is true then the temporary value of X is set equal to the sum of some fraction, A, times X (I,J-1) and some fraction, B, times X (I,J), where B=1 -A and A must be less than one. This is shown more clearly below.

$$TEMPX = A*X(I,J-1) + B*X(I,J) \tag{3.1}$$

where

$$A + B = 1.0 \quad \text{and} \quad A>0 \ , \ B>0$$

After the field has converged, this constraint is removed and final convergence is then obtained in one or two additional iterations. This technique should produce coordinate lines as shown in Figure 3b.

Another problem which was encountered is determining in which arrangement the two bodies should be transformed from the physical plane to the transformed rectangular plane. There are many and varied combinations in which the arbitrary cuts may be placed and where the bodies and reentrant segments may be placed on the transformed plane. In this research an NACA 64_3-418 airfoil and

flap were used for experimentation. Both airfoil and flap had 57 points each describing the body coordinates. Seven different combinations were attempted in order to find a suitable coordinate transformation. Only two of the seven showed any signs of success.

The first case to show promise is shown in Figure 4. Figure 4b shows the airfoil and flap combination in the physical plane encircled by an outer boundary which is at a radius of 10 chord lengths. Also shown as dotted lines are the arbitrary cuts. Figure 4a shows the airfoil combination on the transformed plane. Note that the flap was cut into two pieces and they were placed on the $\xi = 1$ and $\xi = 57$ coordinate lines. Infinity lies on the $\eta = 1$ line and the large airfoil lies on $\eta = 57$ line. The reentrant segments lie above and below the flap. This case was not run to convergence, but to only 320 iterations. The optimum accleration parameter in this case was found to be $\delta = 1.4$. By observing Figure 5 the results can be seen. The hole that appears between the two airfoils can possibly be corrected by using coordinate line contraction.

The second case physical plane setup is also shown in Figure 4a. The same airfoil combination was used here and the cuts are also in the same place. However, the placement of the flap segments and reentrant boundaries are different from before as can be seen from Figure 6. The number of points on infinity are also reduced. It may also be observed that by sliding the flap segments down, more η-lines are placed between the two bodies. This case was run to convergence (convergence criteria for x and y

is 0.00001) in 388 iterations. The optimum acceleration parameter was $\delta = 1.8$. The results are shown in Figure 7. Note that the diagonal straight lines on the plot are not part of the coordinate system but are truncation lines caused by the plotter used.

IV. COMPLEX VARIABLE TRANSFORMATION

Since the previous attempts at achieving a good two-body coordinate system were not very successful, a new and different approach was tried. This approach was stimulated by work done by Ives and Liutermoza [3], Ives [4], and Grossman and Melnik [5] . All three cases involved transonic flow over two-element airfoil systems. In all cases a form of conformal mapping was utilized. This mapping technique caused the infinity boundary to be mapped to a single point and caused the smaller airfoil to be mapped inside the larger airfoil in the transformed plane. Then by application of a Theodorsen transformation the two concentric bodies were mapped to two circular rings. Then a polar coordinate system was used in which to make calculations in the transformed plane.

By observing this technique already developed, a similar but different method was developed that utilized the body fitted coordinate system previously discussed instead of a polar coordinate system.

The first step in this new technique is to utilize a similar mapping function that was used by Grossman and Melnik. This equation is refered to as the complex variable transformation equation.

$$\zeta = \frac{1}{Z + C} \tag{4.1}$$

where
$$\zeta = X_T + iY_T \tag{4.2}$$
(in the transformed physical plane)

$$Z = X_O + iY_O \tag{4.3}$$
(in the original physical plane)

and
$$C = C_R + iC_I \tag{4.4}$$
(a complex constant with real and imaginary parts)

It was determined during the experimentation that C had very little control over the resulting coordinate system and was therefore dropped from the original equation. The final transformation equation was therefore,

$$\zeta = \frac{1}{Z} \tag{4.5}$$

It is readily seen that as $Z \to \infty$, $\zeta \to 0$. Therefore, any infinity boundary is being transformed to a point in the transformed physical plane. If the infinity boundary is taken to be some finite size(i.e. a circle with a radius of 100 chord lengths), then it must be transformed along with the two airfoil elements. The result will be a very small circle in the transformed physical plane, instead of a unique point. This may be more desirable if a potential flow solution is being sought.

Now that the bodies and outer boundary have been transformed, the new transformed body coordinates are read into the body-fitted coordinate system program. The order in which the individual points on each body are read into the computer program has to be determined for each individual setup of airfoil combinations.

This technique will be discussed in more detail later in a case by case study. The coordinate system program is now run to convergence with convergence criteria being 0.00001.

This coordinate system in the transformed physical plane must now be converted to the original physical plane by use of a reverse transformation. The reverse transformation is obtained by evaluating equation (4.5) for Z.

$$Z = \frac{1}{\zeta} \tag{4.6}$$

The values of X_T and Y_T are known for every ξ,η point in the field. By substituting these values into the above equation, the original physical plane coordinates can be calculated as follows.

$$X_O = \frac{X_T}{X_T^2 + Y_T^2} \tag{4.7}$$

$$Y_O = \frac{-Y_T}{X_T^2 + Y_T^2} \tag{4.8}$$

The final coordinate system in the physical plane can now be plotted and stored for further use.

This process of finding a multi-element airfoil coordinate system is listed below in a step by step method. These steps can be seen figuratively in Figures 8,9,11,and 12.

STEP 1. Determine the arrangement of the bodies to be investigated and the type of outer boundary to be used. A typical

arrangement is shown in Figure 8. The order in which the points describing each body are to be read in must be determined here also. The point spacing on each body must also be determined.

STEP 2. Use equation (4.5) and transform the bodies and outer boundary to the transformed physical coordinates. Figure 9 shows a representative transformation from Figure 9.

STEP 3. Determine how this new system is to be placed on the transformed rectangular plane by identifying the cuts (reentrant segments). Input these transformed coordinates to the body-fitted coordinate system program and run the program to convergence. This coordinate system can be seen in Figure 11. If at this point the plot of the coordinate system shows coordinate line spacing not to be very good or if there are overlapping coordinate lines, then a return to Step 1 will be necessary in order to readjust the point spacing on the bodies or the order in which the points are read into the program.

STEP 4. Use equation (4.6) to transform the coordinate system obtained in Step 3 to the final coordinate system in the original physical plane. The final result will appear as shown in Figure 12.

This type of approach has proved very successful and showed much better results than any other approach that was tried. Three different configurations of airfoils were set up and coordinate systems for each were obtained. Each individual case had its own peculiarities and therefore required different techniques

to obtain a desirable result. The three separate cases are described in detail as follows.

CASE 1.

The airfoil elements that were investigated in this case comprised a wing-flap combination with an outer boundary of infinity. The airfoil used for both the wing and flap was an NACA 64_3-418 airfoil. The main airfoil and flap had 57 coordinate points each describing the individual airfoils. Figure 8 shows this wing flap combination.

This two-body system was then transformed to the transformed physical plane. This transformed wing-flap can be seen in Figure 9. It should be noted that the flap now lies within the boundaries of the larger wing. Also infinity now becomes a point ($x = 0$, $y = 0$) as represented by the small x in the figure. Next note that the cuts are placed from the leading edge of the wing to infinity and from infinity to the trailing edge of the flap. Figure 10 shows where the wing, flap, and infinity lie in the transformed rectangular plane.

This setup was run to convergence in 1900 iterations with $\delta = 1.2$. A plot of the transformed physical plane coordinates is shown in Figure 11 . Initially there were problems with overlapping coordinate lines occurring at the sharp trailing edge of the wing. This problem was overcome by using the method described in Chapter III. The coordinates were then transformed to the original physical plane. Figure 12 shows the physical

plane. Figure 12 shows the physical coordinate system. The crossing lines on the plot are not part of the coordinate system and should be disregarded. Figure 13 shows a blowup of the region between the wing and flap. The coordinate lines are concentrated very well in this region as well as being nicely spaced. This will be necessary in order to obtain an accurate solution to any flow problem.

CASE 2.

The airfoil elements that were investigated in this case were also a wing-flap combination. The wing in this case was a modified NACA 64_3-418 airfoil. The modification in this airfoil is in the area of the trailing edge. The flap is also a NACA 64_3-418 airfoil but it is placed much closer to the wing than the flap was in Case 1. The infinity boundary is a circle with a radius of 100 chord lengths. Both wing and flap segments have 57 coordinate points each. The outer boundary has 20 coordinate points. Figure 14 shows this wing-flap configuration without the outer boundary. The transformed physical plane diagram is shown in Figure 15. The corresponding transformed rectangular plane diagram is shown in Figure 16. Figure 15 shows that the flap lies within the boundary of the wing and the outer boundary appears as a small circle within the bounds of the wing.

The overlapping of ξ coordinate lines at the trailing edge of the wing proved to be very troublesome in early trial runs. It was soon learned that this problem could be resolved by adj-

usting the point placement and spacing on the two bodies. This problem and the technique used to correct it can be understood more by referring to Figures 17 and 18. Figures 17 and 18 show the trailing edge portion of the wing and the entire flap. Region A, the curved portion of the trailing edge of the wing, and region B, approximately the front one third surface of the flap, are the regions of interest. It was determined that there needed to be the same number of coordinate points in region A as there were in region B. In the original setup A had much fewer points than B since there was a high concentration of points on the leading edge of the flap. Because of this many of the points on the leading edge of the flap were connected by ξ-lines bent very sharply around the sharp trailing edges of the wing. The bend that was required was too sharp and overlapping of these ξ-lines resulted. An example of this type of overlap can be seen in Figure 17.

To correct this situation more coordinate points were added to region A and some points were removed from other areas of the wing to maintain the original 57 points describing the wing. Likewise some points in region B were removed and placed somewhere else on the flap. An example of the resulting non-overlapping of ξ-lines can be seen in Figure 18. This technique proved very effective in eliminating overlap.

Once the overlap problem was overcome the coordinate system was converged in 1823 iterations with $\delta=1.2$. The converged transformed physical plane plot is shown in Figure 19. The

original physical plane plot is shown in Figure 20. In this figure the coordinate lines extending to the outer boundary have been cut off the plot in order to enhance the size of the wing and flap. Figure 21 shows a blowup of the region between the wing and flap. This coordinate system should prove to be very effective in helping to generate solutions to actual flow problems.

CASE 3.

The airfoil configuration investigated in this case is a NACA 64_3-418 wing and a slat that was created by the author. The infinity boundary is taken to be a circle of radius of 100 chord lengths. Both wing and slat have 57 coordinate points each. Figure 22 shows this wing-slat configuration without the outer boundary. The transformed physical plane diagram is shown in Figure 23 and the corresponding transformed rectangular plane diagram is shown in Figure 24.

Overlapping ξ and η lines at the trailing edge of the slat were prominent in early test runs. The ξ-line overlap was corrected by placing the arbitrary cuts in different places. In effect, all this amounts to is changing the order in which the points on the body are arranged on the transformed rectangular plane. This was accomplished by reading the points describing the body into the body-fitted coordinate system program in a different order. In this case the order of the points on the slat were changed. Originally the points were read in from the leading edge going in a clockwise direction around the airfoil. It was determined that the 15th point from the leading edge on the top

of the slat would be a better starting point to input the slat coordinate points. In Figure 23 the cut from the infinity circle to the slat touches the slat on the top surface of the slat(In the transformed physical plane the top of the slat lies on the bottom side.)instead of at the leading edge as it did originally. This procedure corrected the ξ-line overlap and gave a much better ξ-line distribution.

The η-line overlap was resolved by using the technique described in Chapter III of forcing the lines not to overlap by controlling the temporary iterative values of both X and Y. Figure 25 shows the trailing edge of the slat in the transformed physical plane. This plot clearly shows the η-lines overlapping the trailing edge. Figure 26 shows how the trailing edge looks after applying the technique to remove the overlap. The results of this procedure are very encouraging.

After these problems were overcome the coordinate system was run to convergence in 1629 iterations with δ=1.2. The converged transformed physical plane plot is shown in Figure 27. The original physical plane plot is shown in Figure 28 and a blow-up of the region between the slat and wing is shown in Figure 29.

V. CONCLUSIONS AND RECOMMENDATIONS

The two-body coordinate systems generated in the research were generally acceptable. The ones that were unsuccessful were not a total loss. They pointed out the faulty approaches and shed light on new and better methods. In general the coordinate systems generated by using only the body-fitted coordinate system method proved less desirable than the ones generated from the complex variable transformation method. The complex variable method may be a little more time consuming and arduous but the results are usually much better. In all three cases very good results were obtained by using this method.

The complex variable method is by no means perfect. Future studies should be made to determine the optimum positioning of the arbitrary cuts. Research should also be done to determine the best coordinate point positioning for different configurations. Other methods for controlling the overlap problem should also be investigated. There may also be a better type of complex transformation available. Once these methods have been refined and improved, coordinate systems for more than two-bodies may be obtained using these same basic methods.

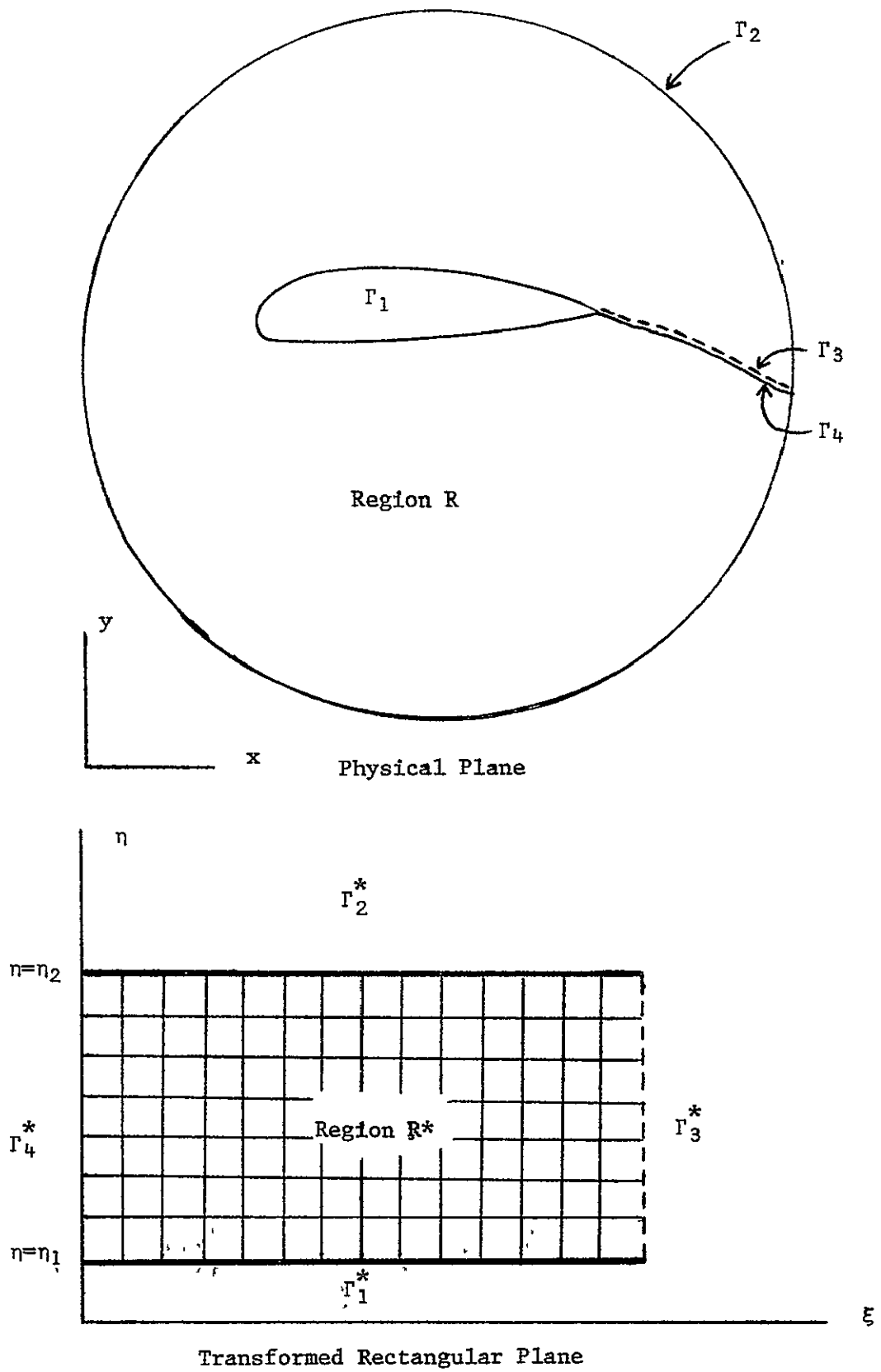

Figure 1. Field Transformation - Single Body

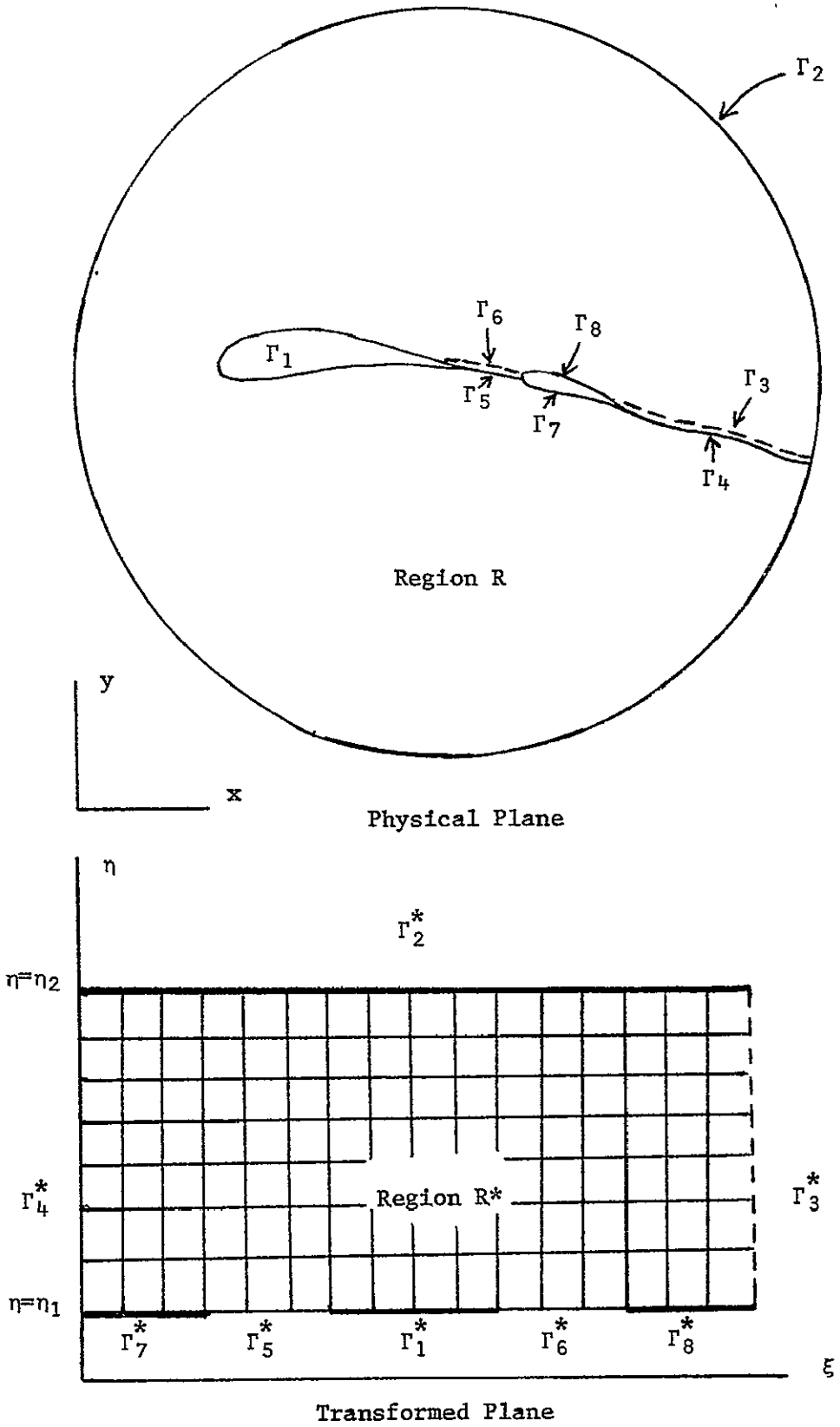

Figure 2. Field Transformation - Two Bodies

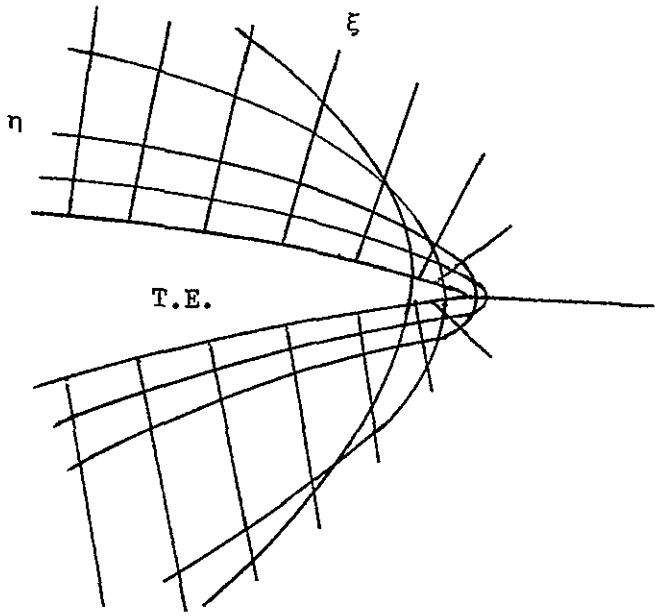

Figure 3a. Airfoil Trailing Edge With Overlapping Coordinate Lines

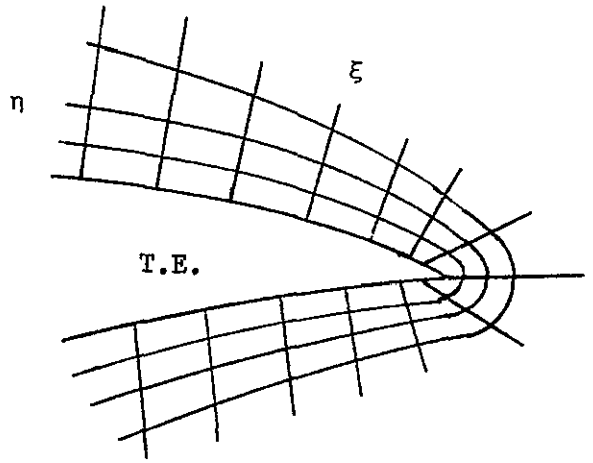

Figure 3b. Airfoil Trailing Edge Without Overlapping Coordinate Lines

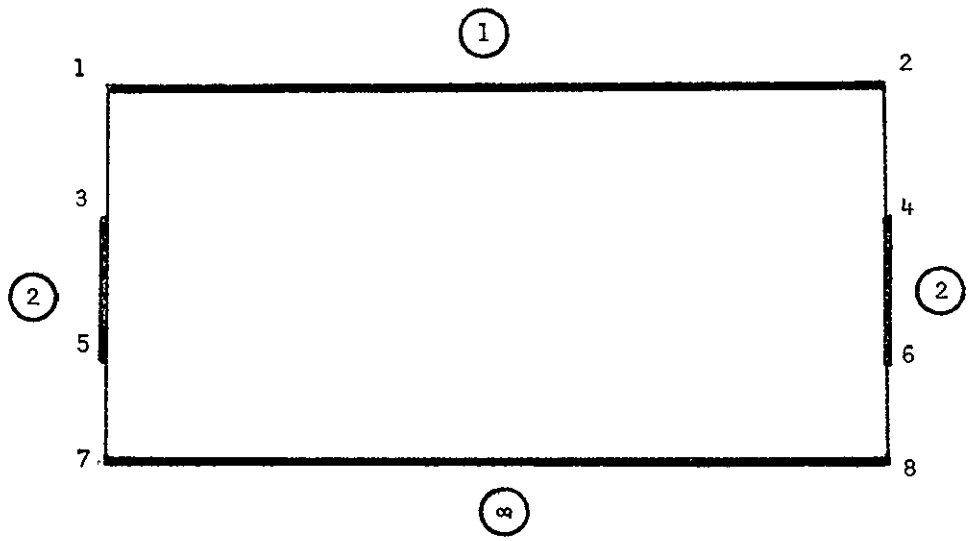

Figure 4a. Transformed Rectangular Plane View of NACA 64_3-418 Wing-Flap Combination (1st Case)

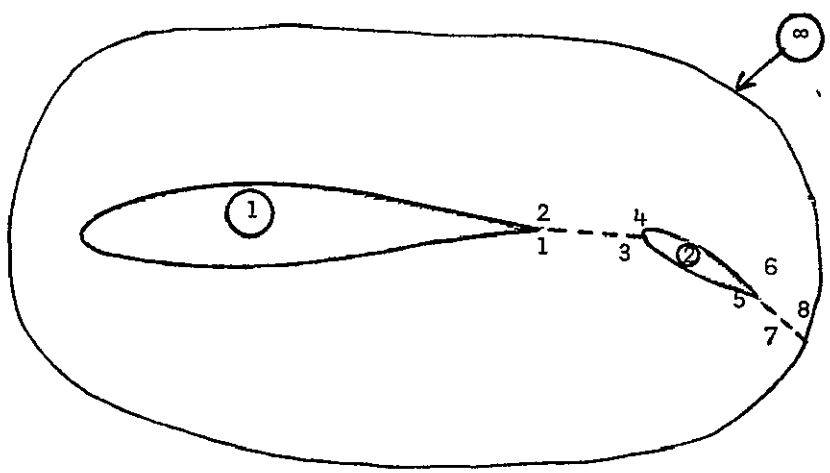

Figure 4b. NACA 64_3-418 Wing-Flap Configuration

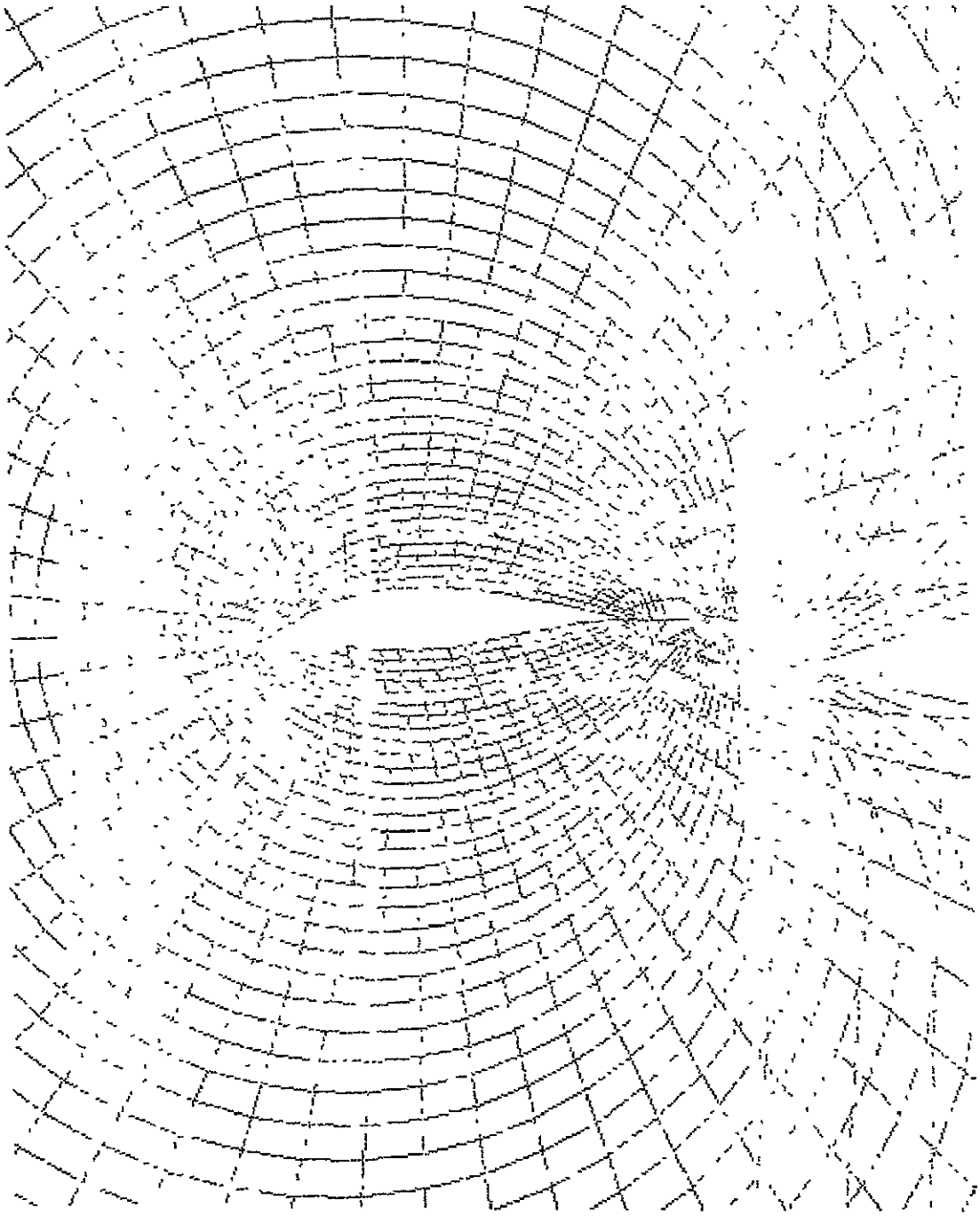

Figure 5. Physical Plane Coordinate System of NACA 64_3-418 Wing-Flap Configuration(1st Case)

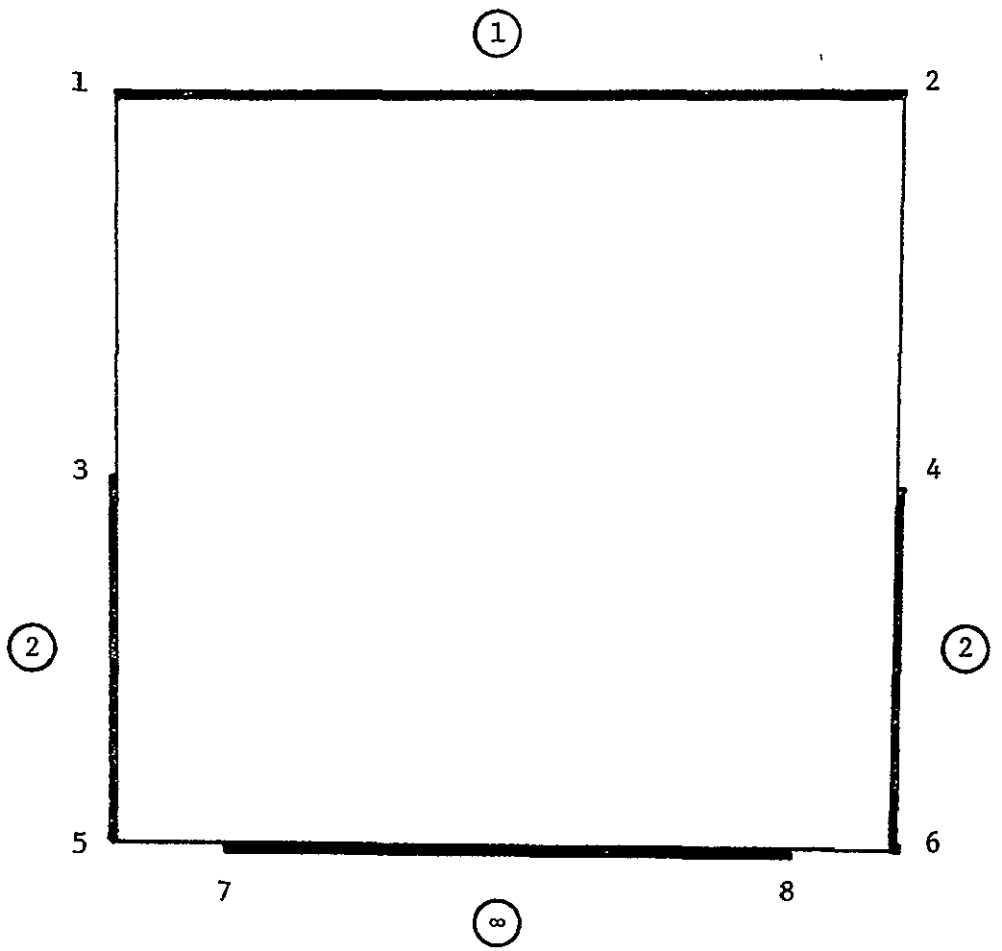

Figure 6. Transformed Rectangular Plane View of $NACA64_3$-418 Wing-Flap Combination (2nd Case)

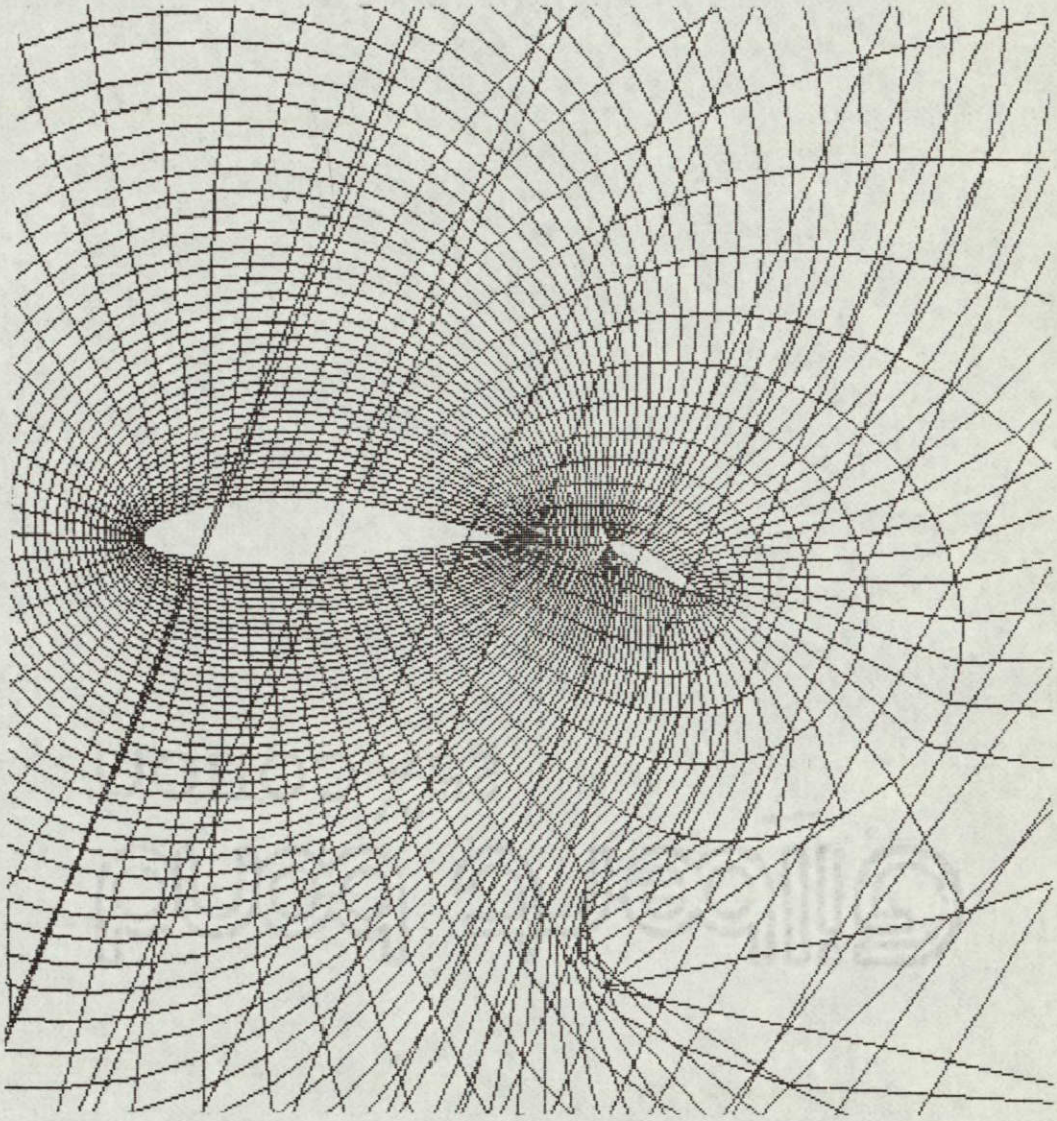

Figure 7. Physical Plane Coordinate System of NACA 64_3-418 Wing-Flap Configuration(2nd Case)

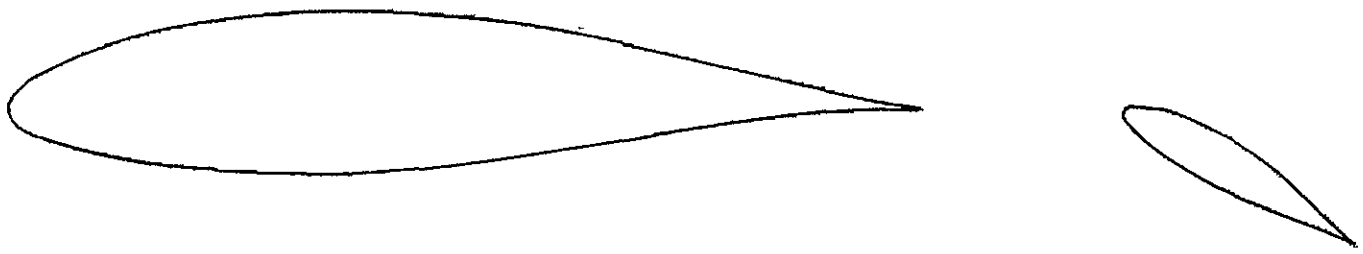

Figure 8. Physical Plane Coordinates of NACA 64_3-418 Wing-Flap Configuration(Enlarged View)

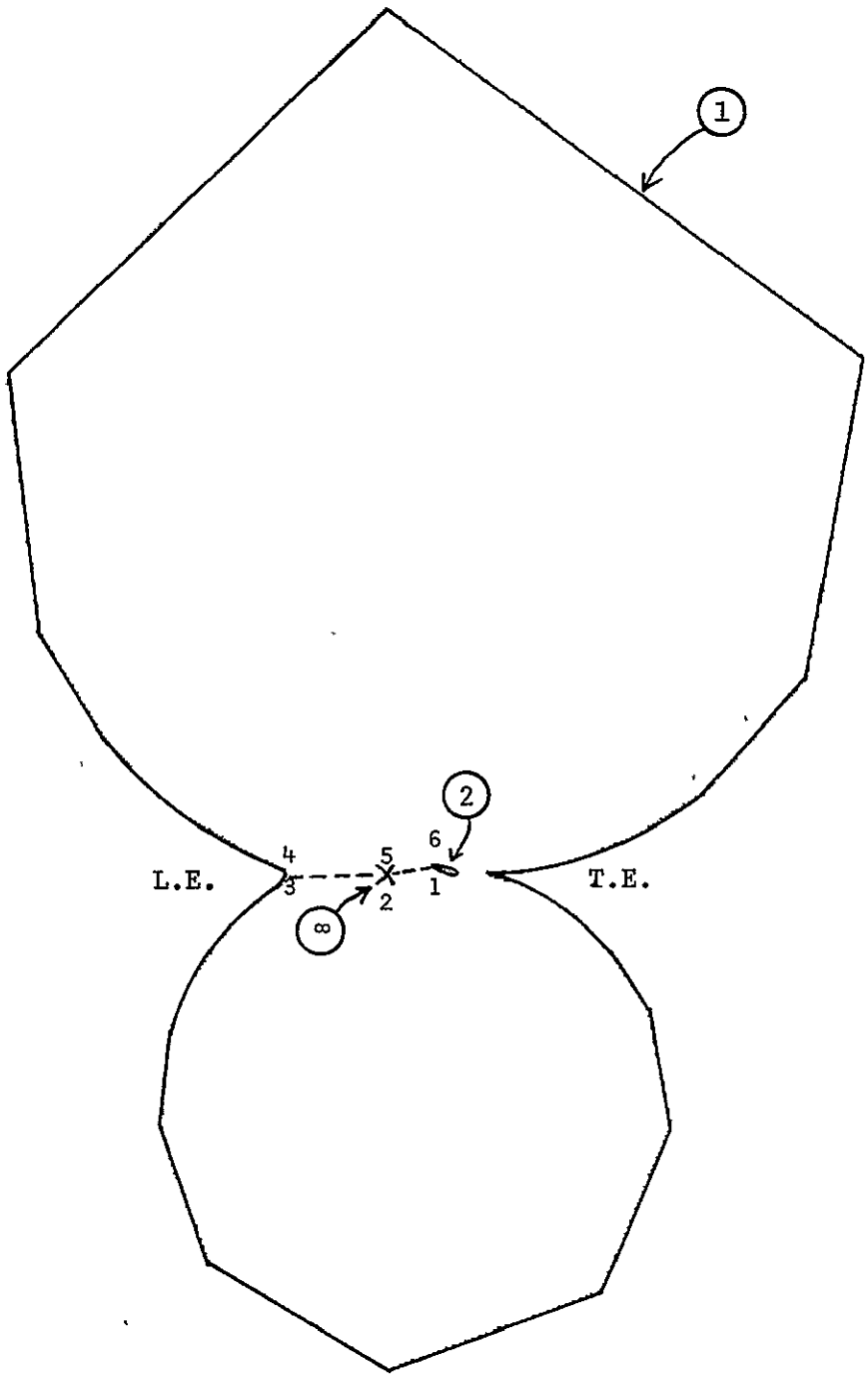

Figure 9. Transformed Physical Plane Coordinates of NACA 64_3-418 Wing-Flap Configuration

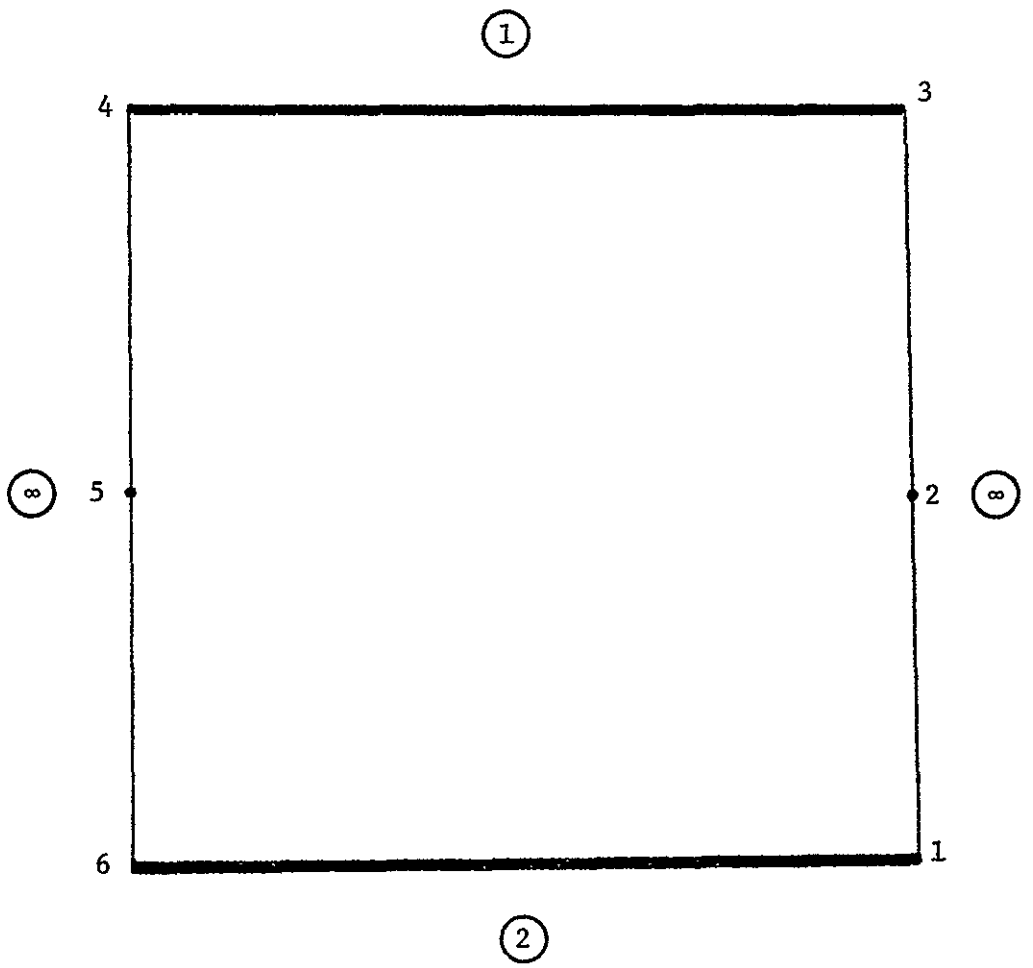

Figure 10. Transformed Rectangular Plane View of Transformed NACA 64_3-418 Wing-Flap Coordinates

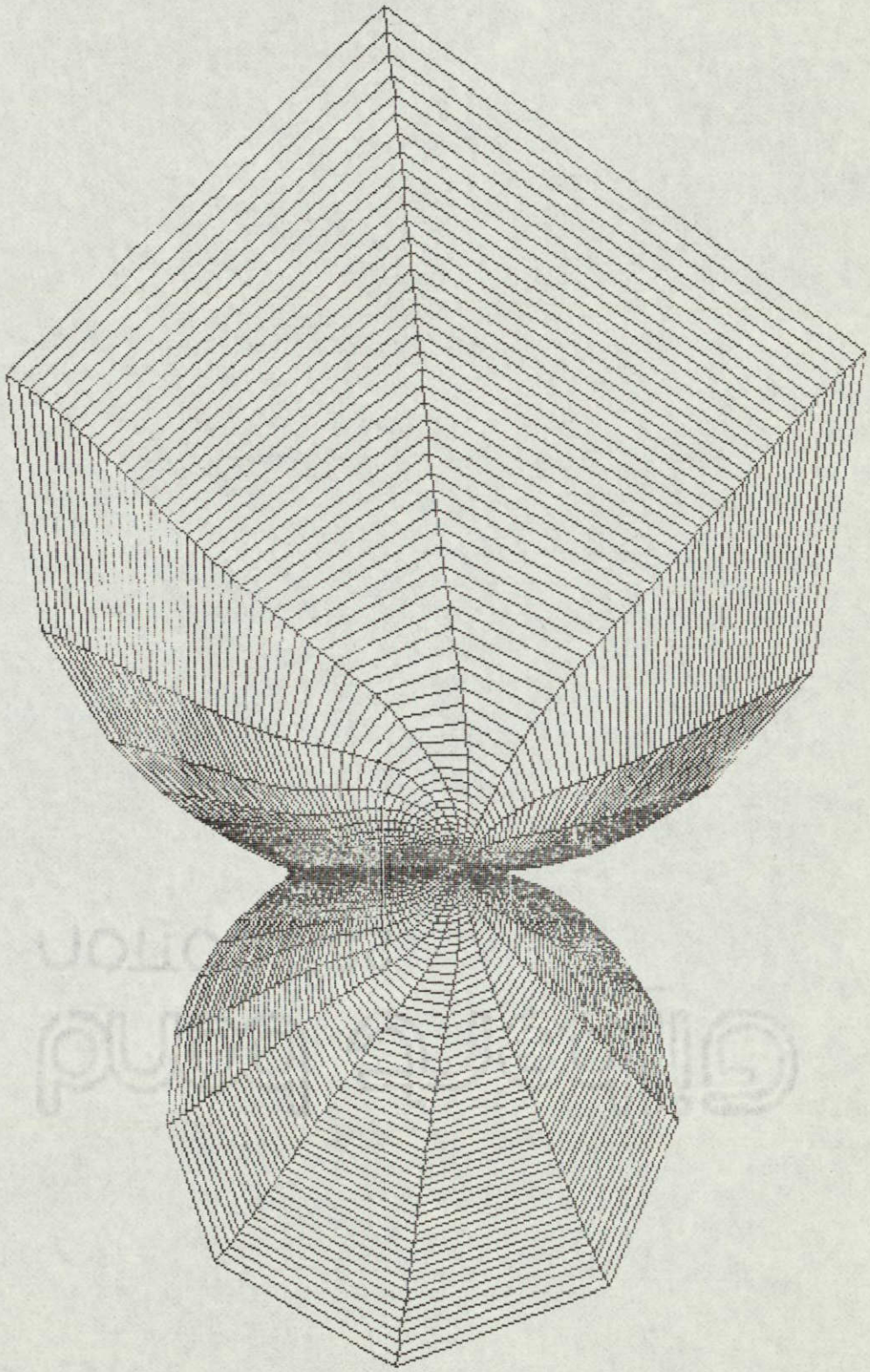

Figure 11. Transformed Physical Plane Coordinate System of NACA 64_3-418 Wing-Flap Configuration

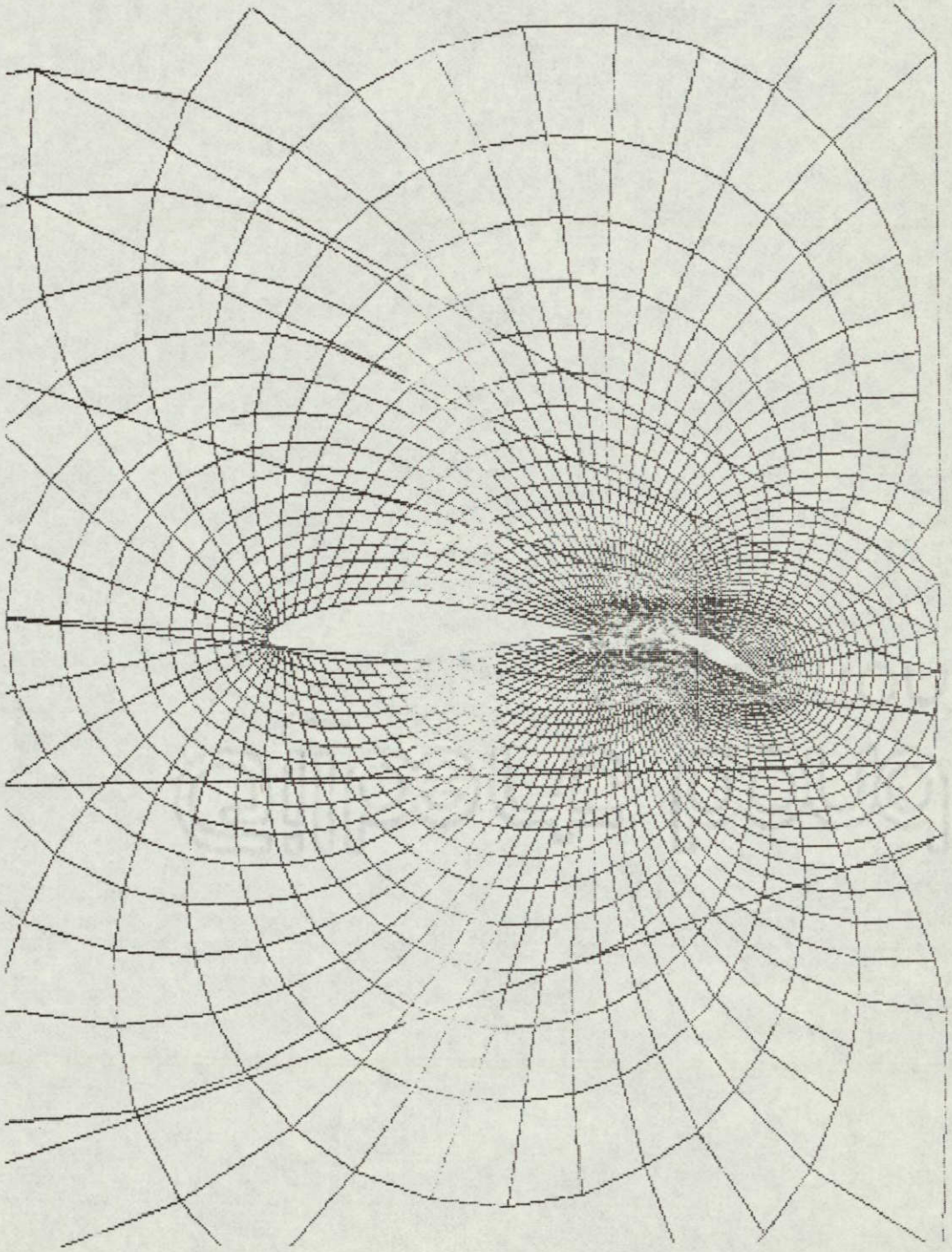

Figure 12. Physical Plane Coordinate System of NACA 64_3-418 Wing-Flap Configuration

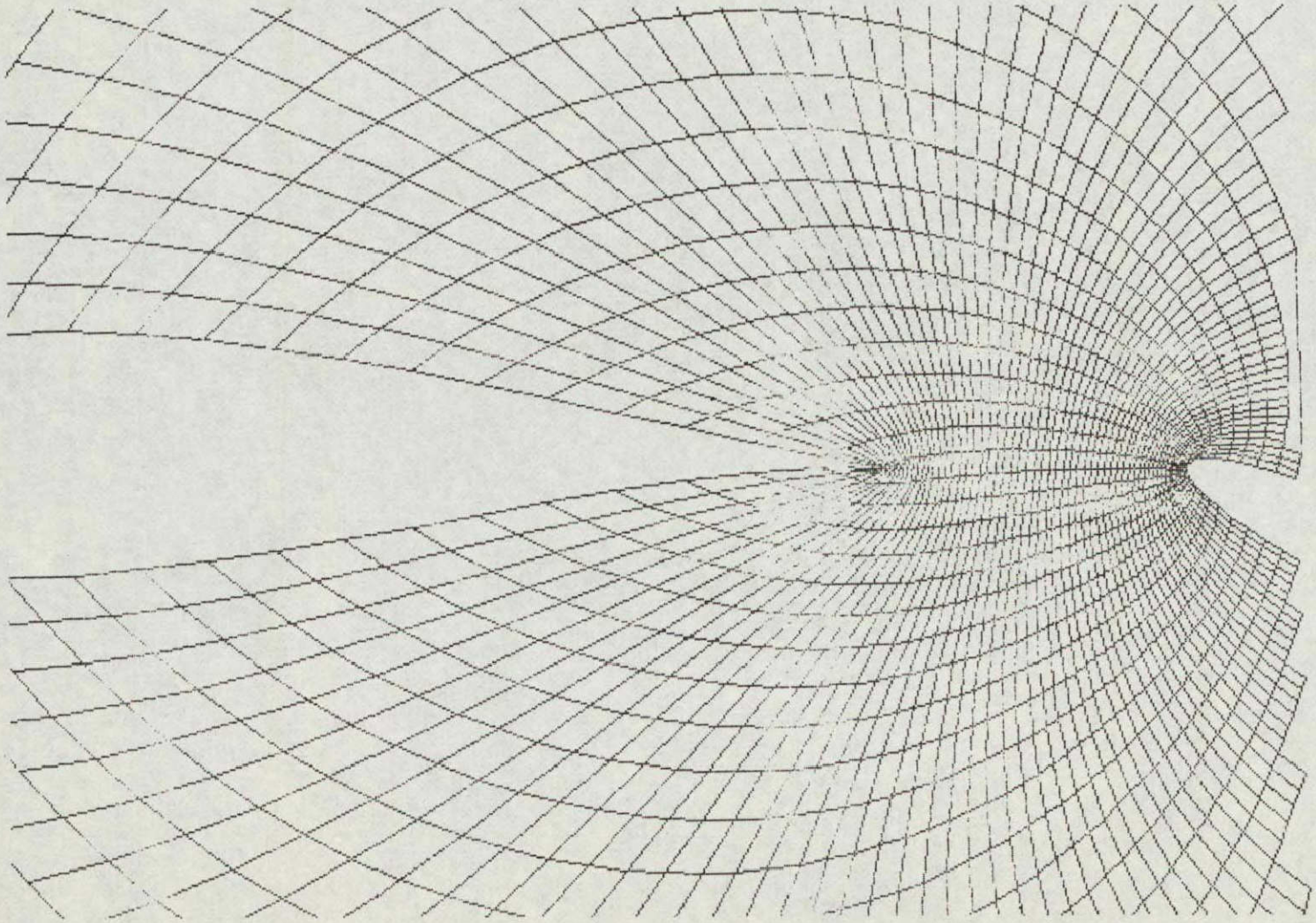

Figure 13. Expanded View of Physical Plane Coordinate System of NACA 64_3-418 Wing-Flap

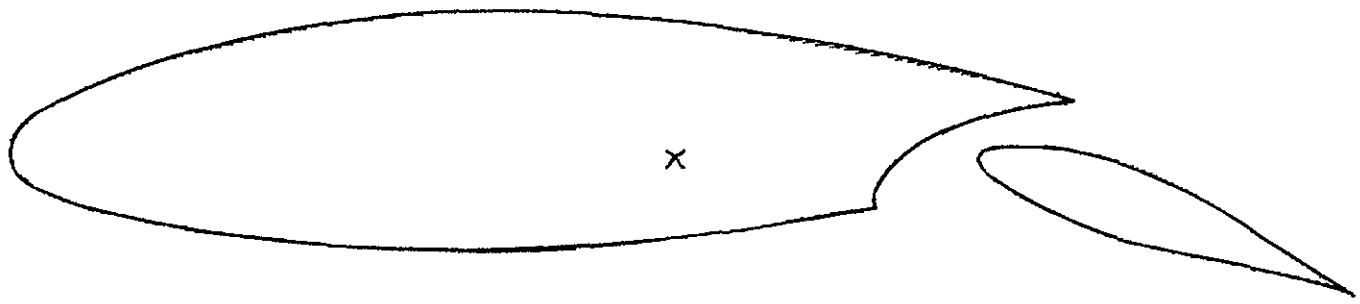

Figure 14. Physical Plane View of Modified NACA 64_3-418 Wing-Flap Configuration

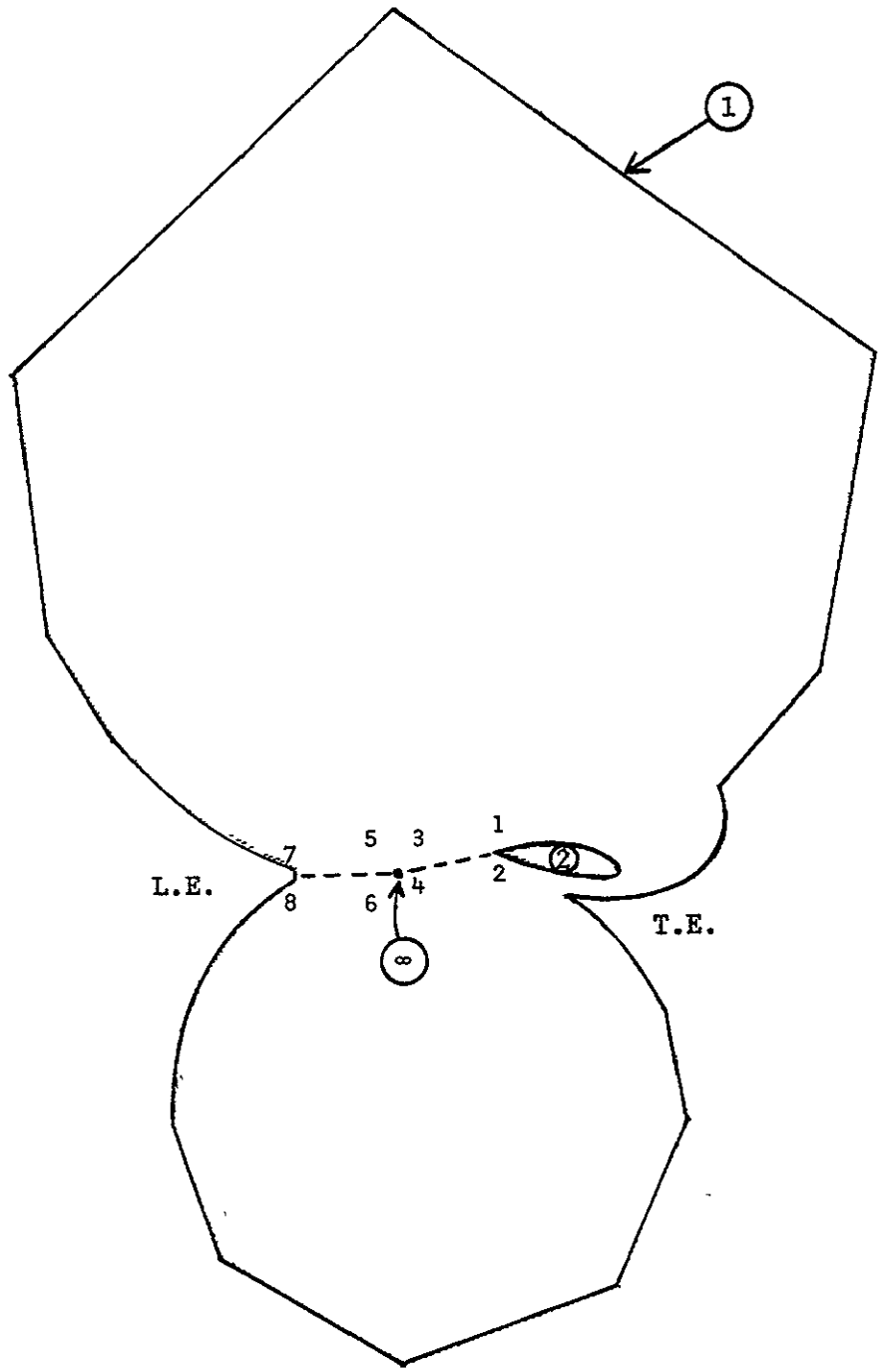

Figure 15. Transformed Physical Plane of Modified Wing-Flap

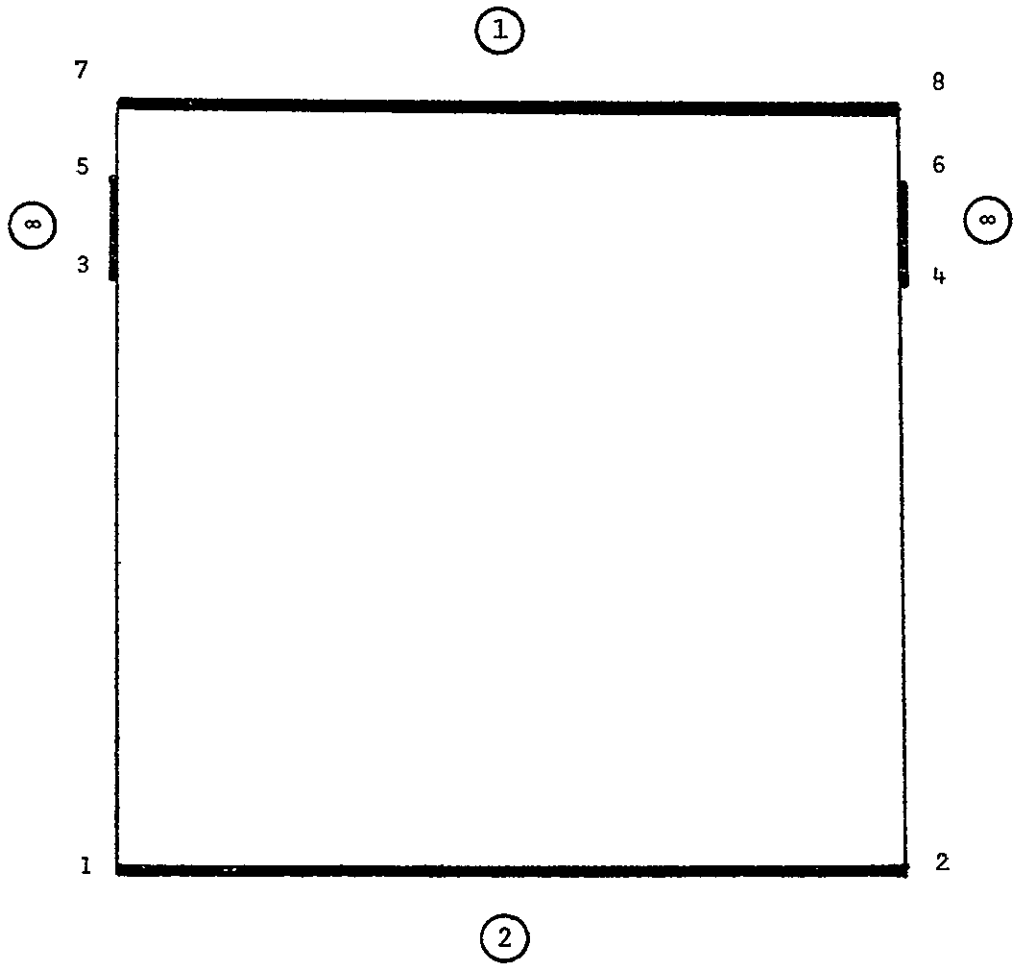

Figure 16. Transformed Rectangular View of Transformed Modified Wing-Flap Coordinates

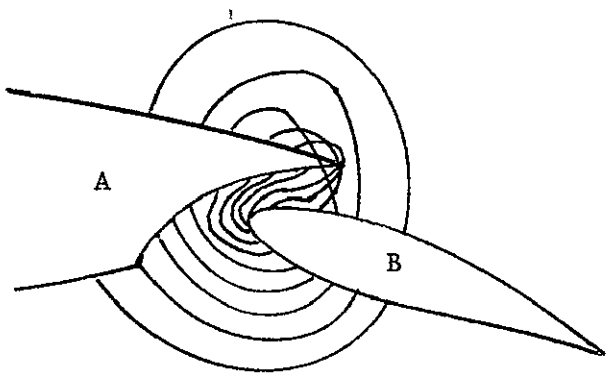

Figure 17. ξ-line Overlap at T.E.

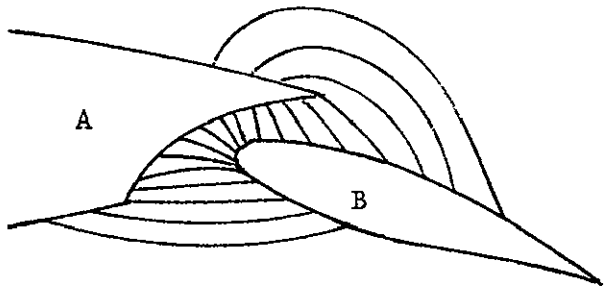

Figure 18. ξ-line Overlap at T.E. Corrected

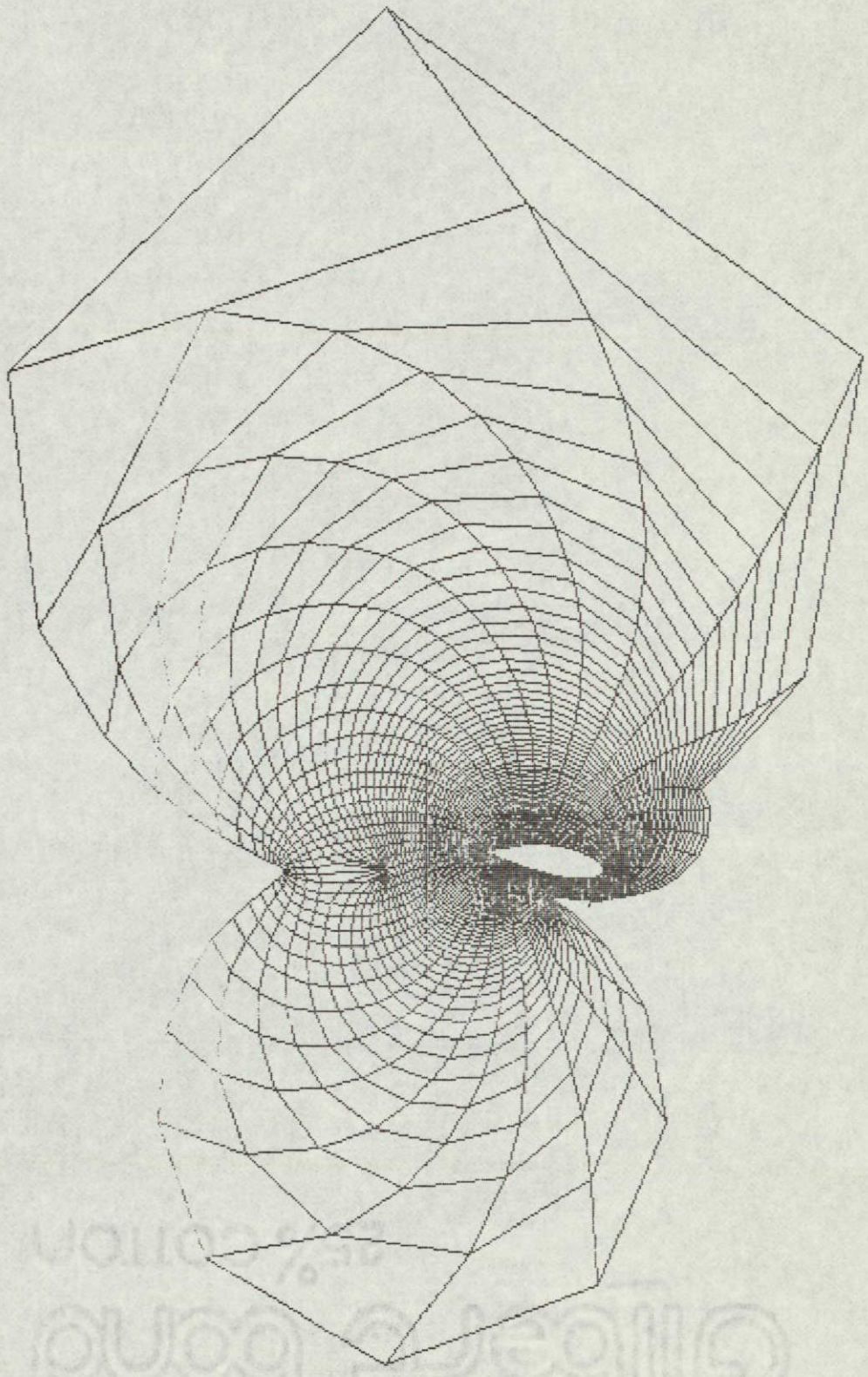

Figure 19. Transformed Physical Plane Coordinate System of Modified Wing-Flap Configuration

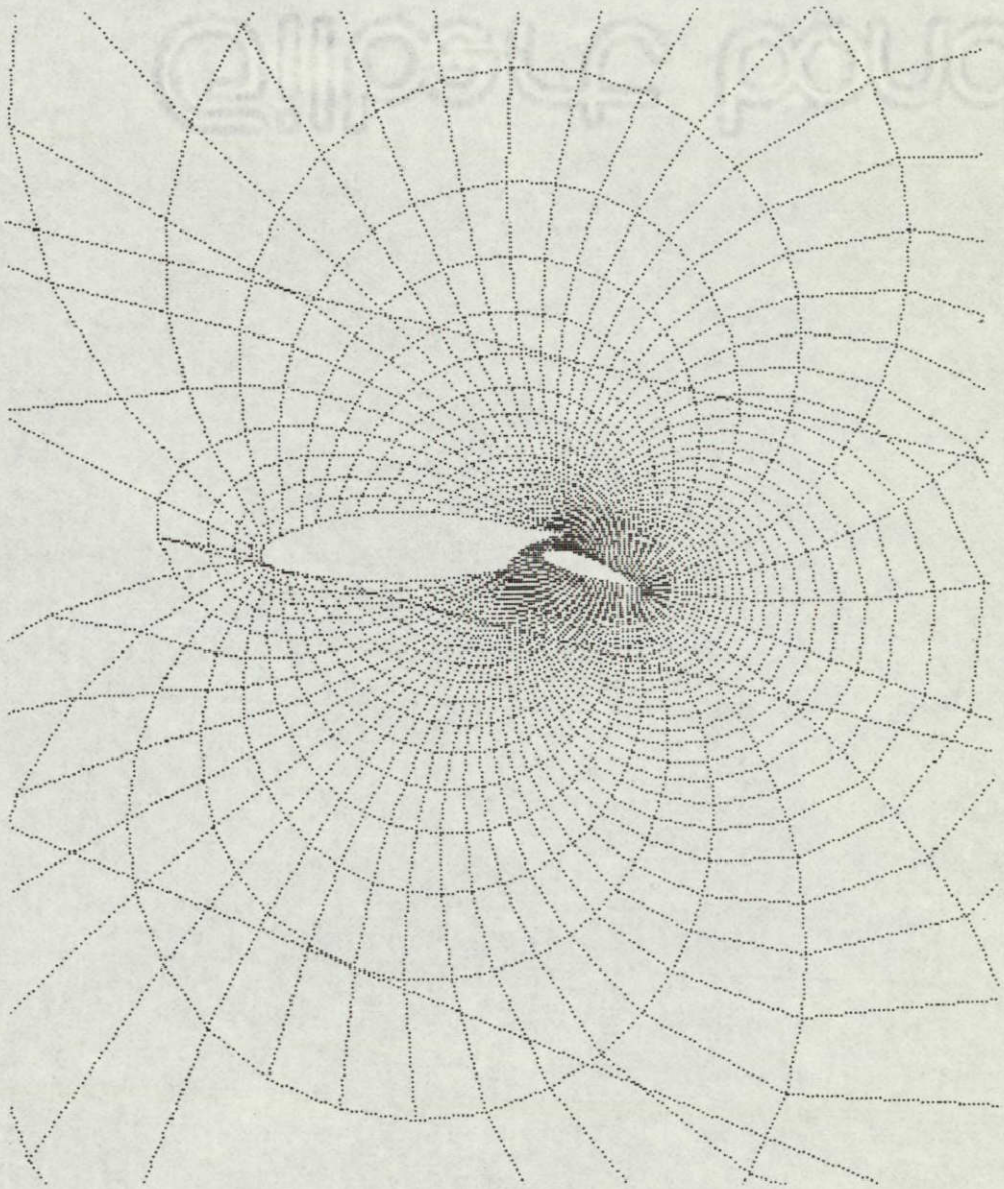

Figure 20. Physical Plane Plot of Modified Wing-Flap Coordinate System

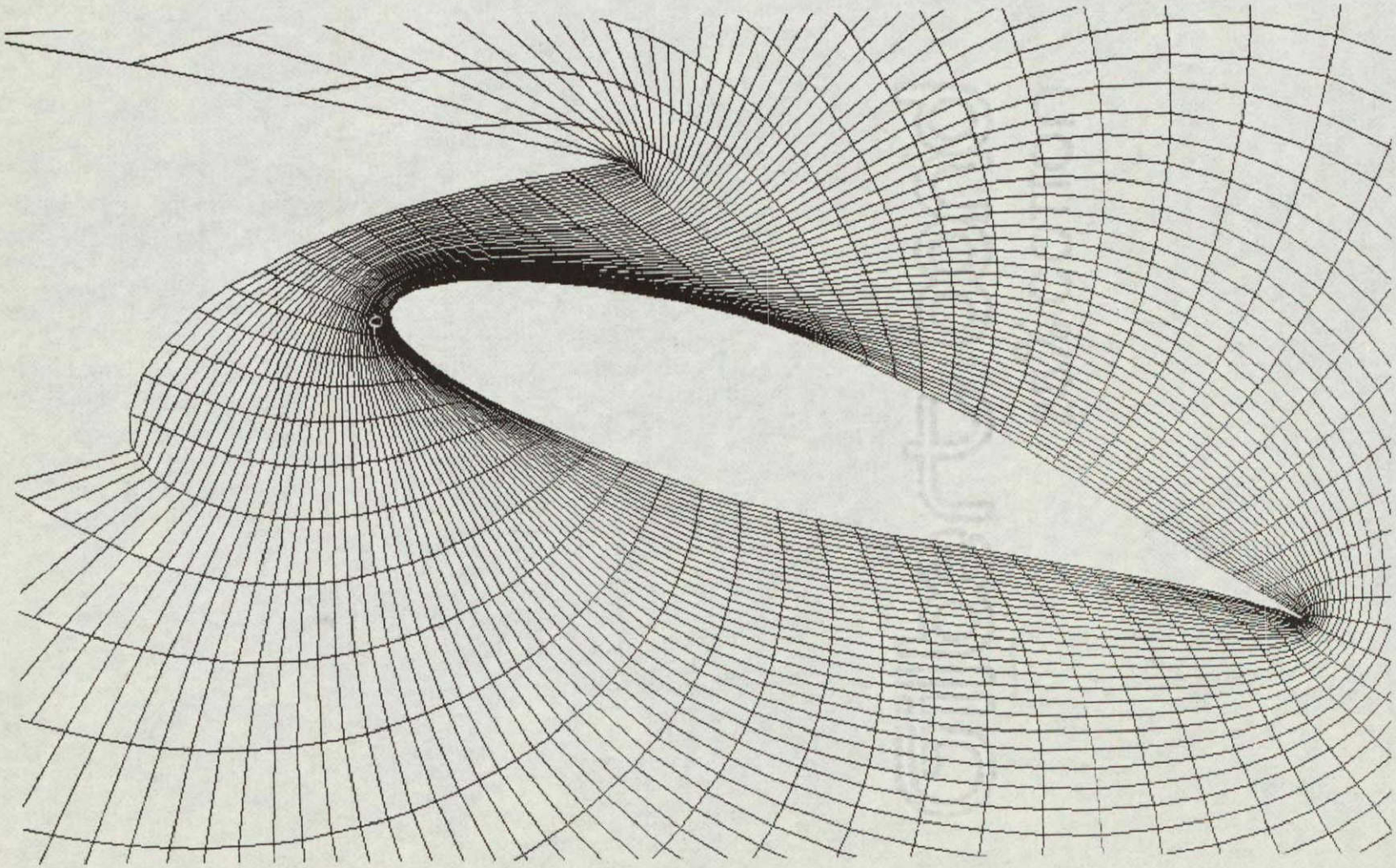

Figure 21. Expanded View of Physical Plane Plot of Modified Wing-Flap Coordinate System

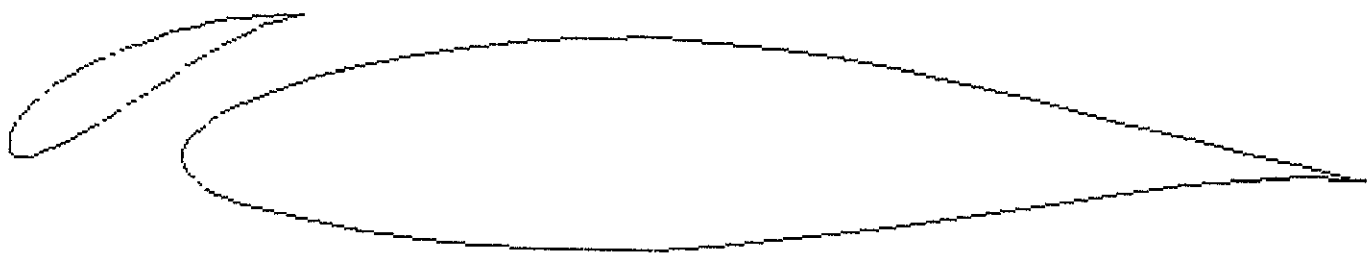

Figure 22. Wing-Slat Configuration

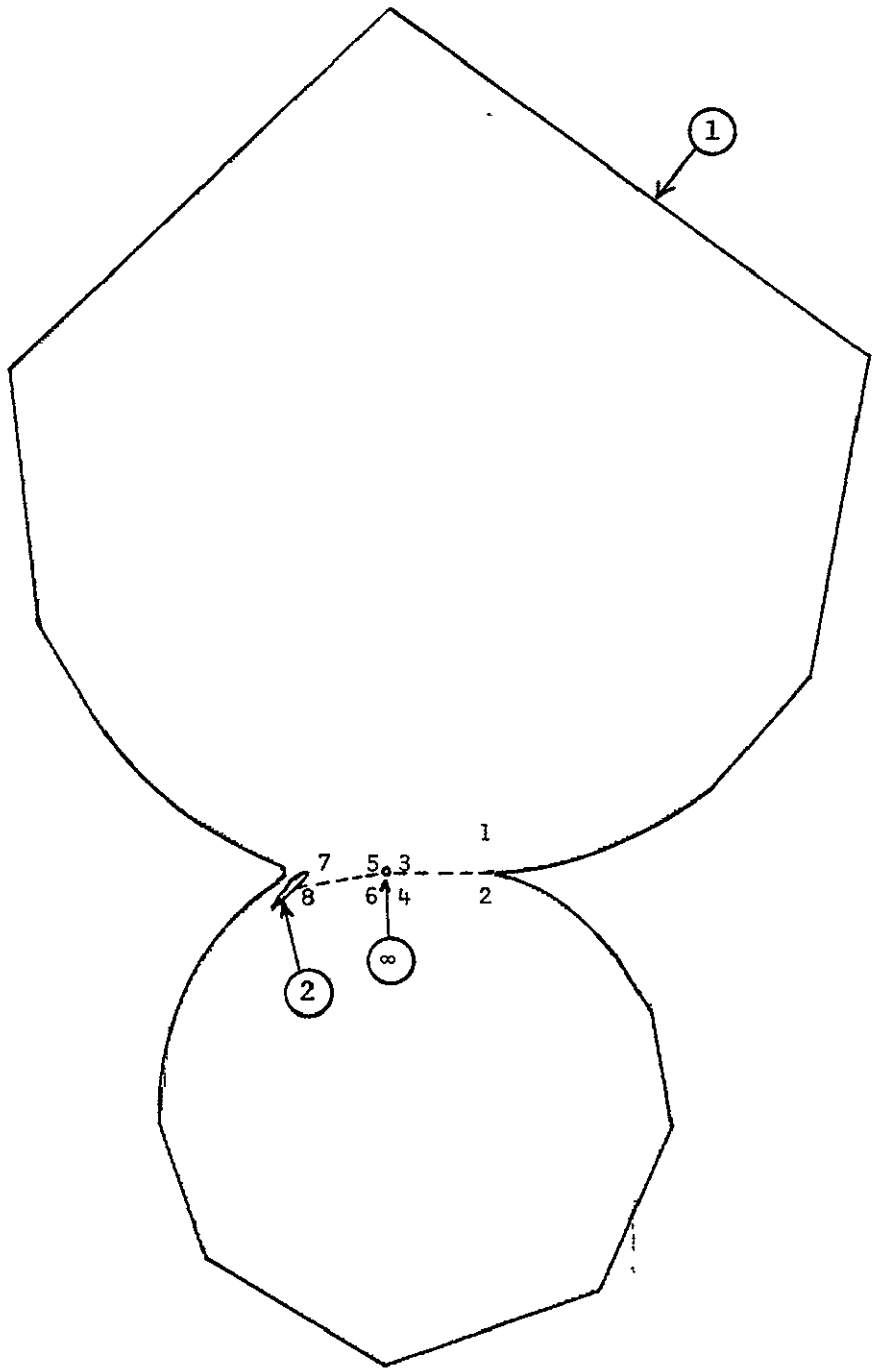

Figure 23. Transformed Physical Plane Diagram of Wing-Slat Configuration

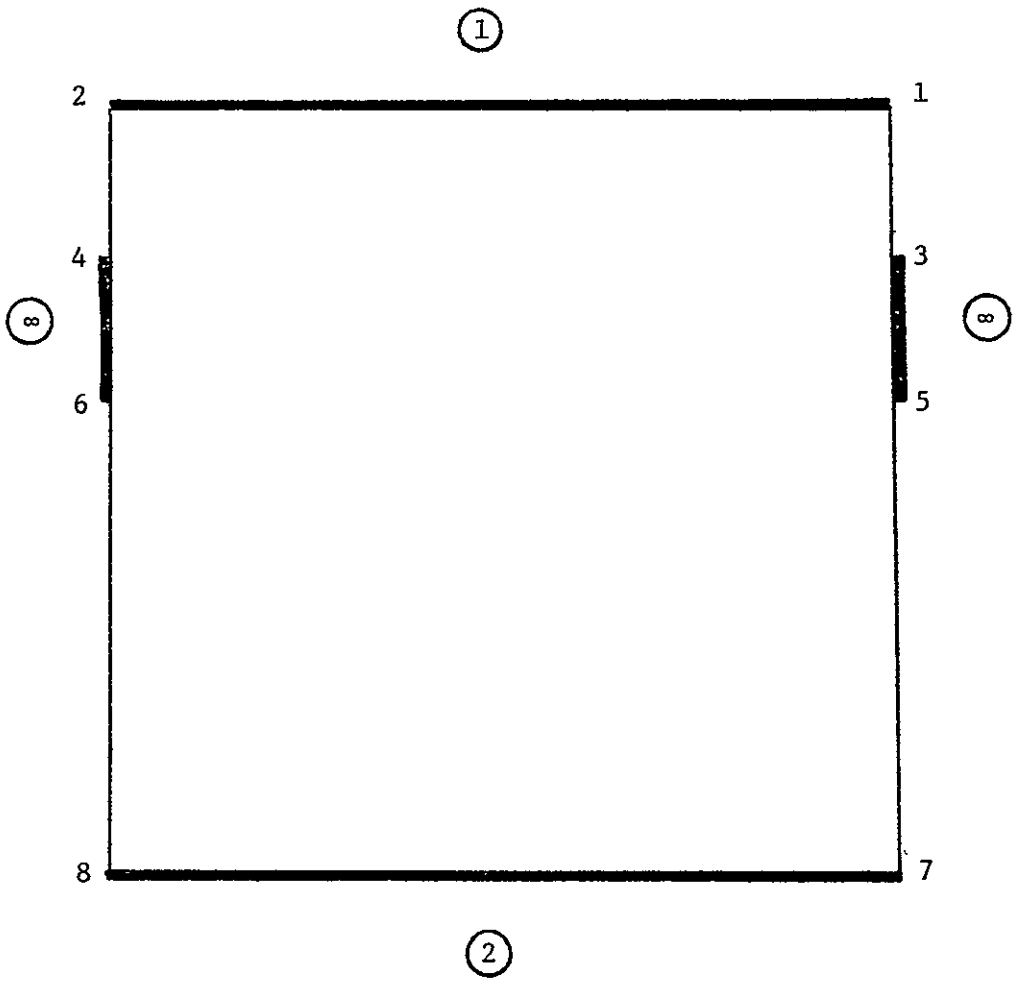

Figure 24. Transformed Rectangular Plane View of Wing-Slat Configuration

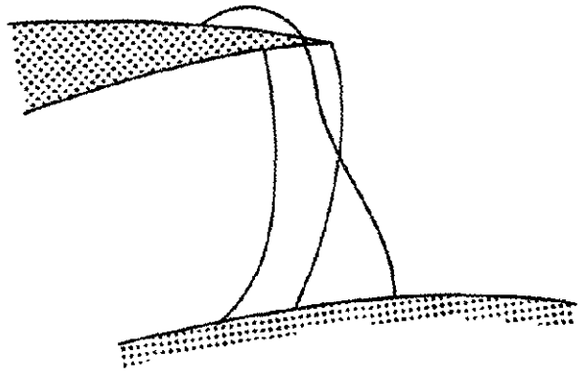

Figure 25. Slat T.E. with η-line Overlap

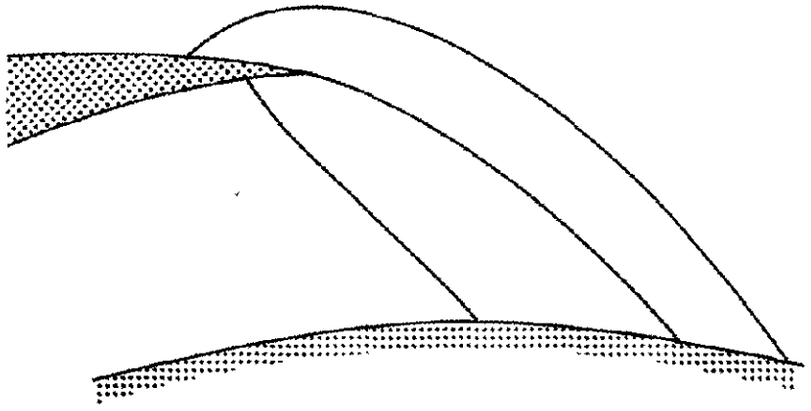

Figure 26. Slat T.E. without η-line Overlap

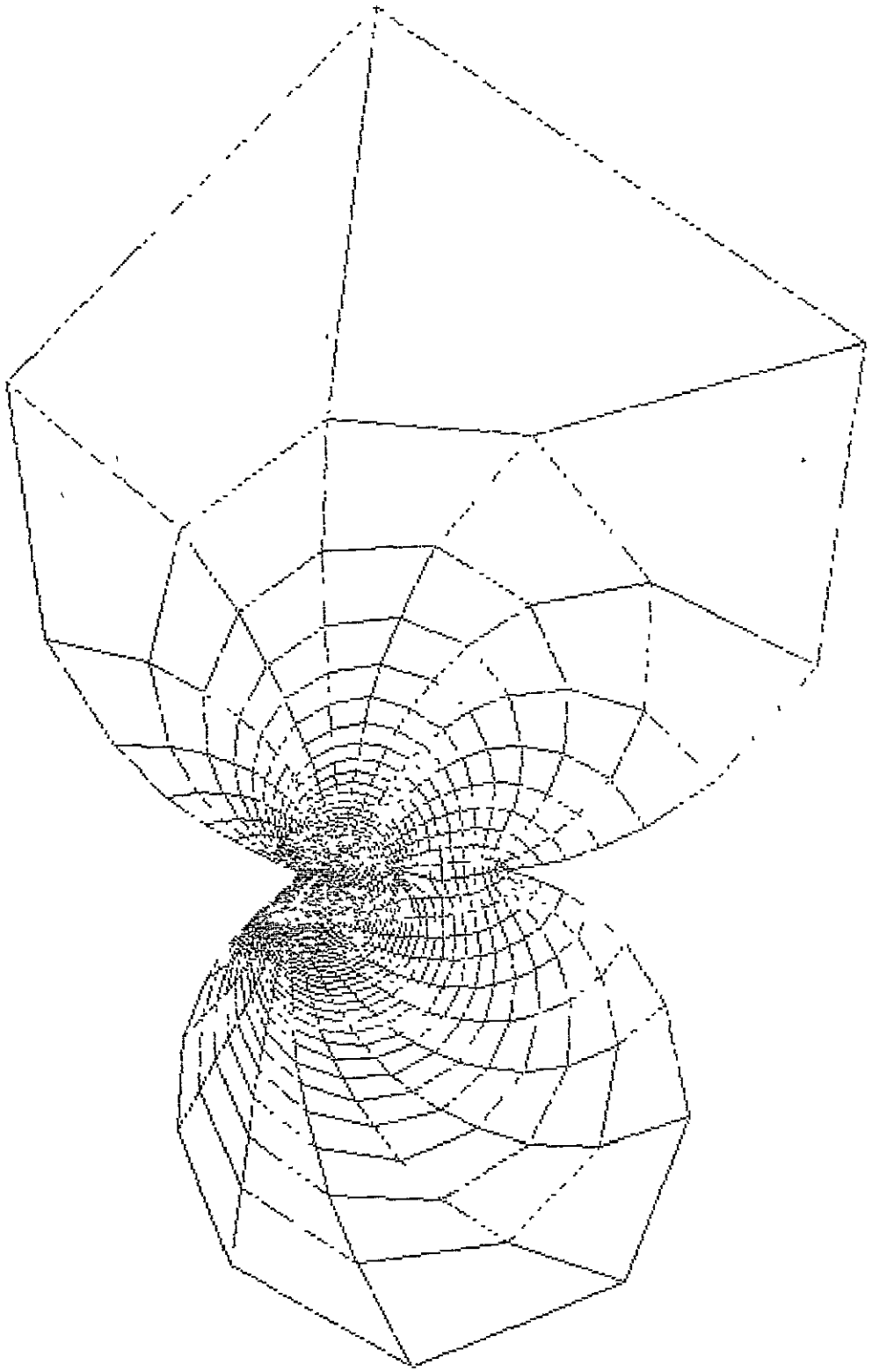

Figure 27. Transformed Physical Plane View of Wing-Slat Configuration

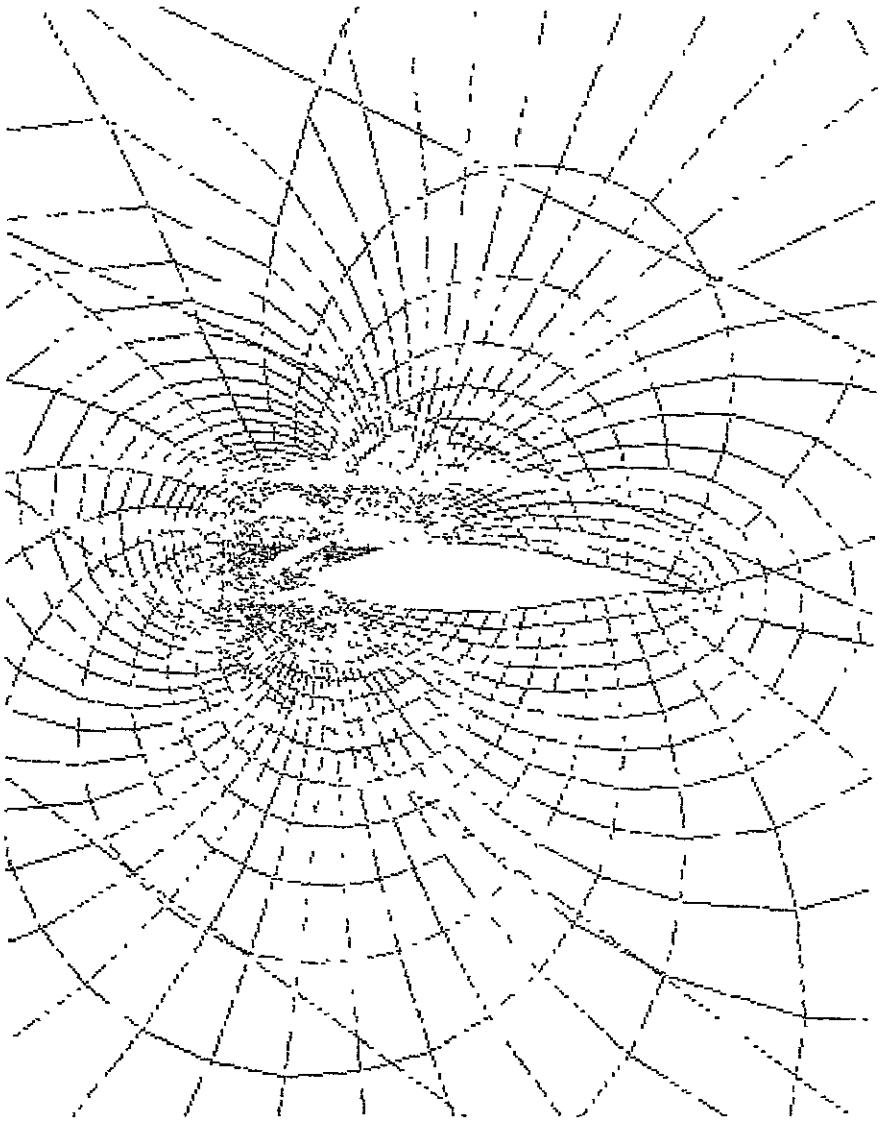

Figure 28. Physical Plane Plot of Wing-Slat Coordinate System

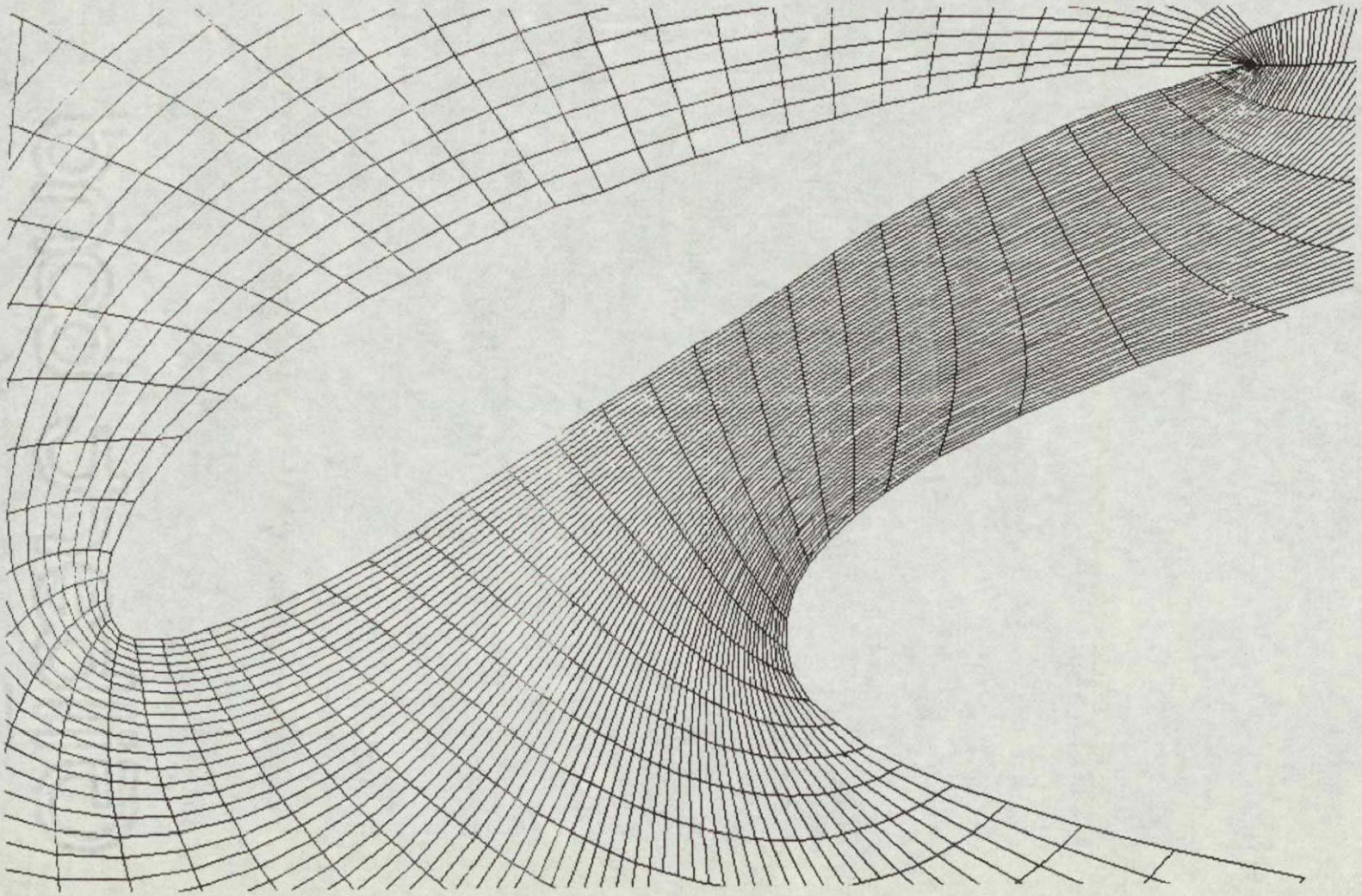

Figure 29. Expanded View of Physical Plane Plot of Wing-Slat Coordinate System

BIBLIOGRAPHY

1. Thompson, J.F., Thames, F. C., and Mastin, C. W., "TOMCAT - A Code for Numerical Generation of Boundary-Fitted Curvilinear Coordinate Systems on Fields Containing Any Number of Arbitrary Two-Dimensional Bodies," Journal of Computational Physics, 24, 274, (1977).

2. Thames, F. C., "Numerical Solution of the Incompressible Navier-Stokes Equations about Arbitrary Two-Dimensional Bodies," Ph.D. Dissertation, Mississippi State University, Mississippi State, Mississippi (1975).

3. Ives, D. C. and Liutermoza, J. F., "Analysis of Tranconic Cascade Flow Using Conformal Mapping and Relaxation Techniques," AIAA Paper No. 76-370 (1976).

4. Ives, D. C., "A Modern Look at Conformal Mapping Including Multiply Connected Regions," AIAA Journal, 14, 8 (1975)

5. Grossman, B. and Melnik, R. E., "The Numerical Computation of the Transonic Flow Over Two Element Airfoil Systems," Proceedings of the Fifth International Conference on Numerical Methods in Fluid Dynamics, Lecture Notes in Physics, 59,220(1976).

6. Thompson, J. F., Thames, F. C. and Mastin, C. W., "Automatic Numerical Generation of Body-Fitted Curvilinear Coordinate System for Field Containing Any Number of Arbitrary Two-Dimensional Bodies," Journal of Computational Physics, 15, 299 (1974).

7. Reddy, R. N., "Numerical Solution of Incompressible Navier-Stokes Equations In Integro-Differential Formulation Using Boundary-Fitted Coordinate System," Ph.D. Dissertation, Mississippi State University, Mississippi State, Mississippi (1977).